Perspective:

Functional Nanoparticles from the Solution Self-Assembly of Block Copolymers

Ulrich Tritschler, Sam Pearce, Jessica Gwyther, George Whittell, and Ian Manners*

School of Chemistry, University of Bristol, Bristol BS8 1TS, United Kingdom

Abstract.

This Perspective outlines recent advances concerning the formation and potential uses of block copolymer micelles, a class of soft matter-based nanoparticles of growing importance. As a result of rapidly expanding interest since the mid 1990s, substantial advances have been reported in terms of the development of morphological diversity and complexity, control over micelle dimensions, scale up, and applications in a range of areas from nanocomposites to nanomedicine.

1. Introduction

The solution self-assembly of block copolymers (BCPs), which consist of covalently linked, and more recently non-covalently linked, macromolecular building blocks, represents an important method for the creation of soft matter-based core-shell nanoparticles (micelles) with useful properties and functions.[1-17] A precisely designed BCP architecture is a key prerequisite for controlling the solution self-assembly process by tuning the interactions between the different polymer segments, both with each other, and the solvent.[1, 6, 18] Well-defined BCPs, such as diBCPs, linear and star triBCPs, are now accessible via a variety of living polymerization techniques, including anionic polymerization and controlled radical polymerization methods, such as reversible addition-fragmentation chain transfer (RAFT) polymerization, nitroxide mediated living radical polymerization (NMP), and atom transfer radical polymerization (ATRP).[19, 20] The discovery of the living anionic polymerization in the 1950s was a key milestone for the preparation of synthetic BCPs[21, 22] and the first solution self-assembly studies on BCPs followed in the early 1960s.[23, 24] More recently, controlled radical polymerization techniques have played a pivotal role by permitting a marked expansion of the range of BCP chemistries and thereby micelle functionality accessible.[25-30]

In this Perspective we focus on recent developments concerning the self-assembly of BCPs in solvents that are selective for one or more of the blocks. After a brief overview of factors that generally influence the micelle morphology and dimensions during the solution self-assembly process (section 2), we focus on different approaches to the formation of BCP micelles. This includes the solution self-assembly of BCPs into micelles with amorphous cores (section 3), as well as micelles with crystalline cores (section 4). In section 5 we discuss the in-situ polymerization and solution self-assembly of amphiphilic BCPs, which is an emerging method for the large scale preparation of BCP micelles. Section 6 focuses on potential applications. Throughout we provide an overview of these topics by the discussion of

selected, representative examples. A discussion of the solution self-assembly of polypeptide amphiphiles, as well as properties and applications of polypeptide-based nanoparticles are beyond the scope of this review and the reader is referred to the relevant literature.[31-36]

2. Factors that Influence Micelle Morphology

The self-assembly of molecular amphiphiles, such as low molar mass surfactants or lipids, to yield micelles in water is mainly driven by the increase in entropy associated with the expulsion of solvating molecules.[37] This enables the insoluble hydrophobic tails of the amphiphiles to aggregate, thereby minimising enthalpically unfavourable hydrophobe-water interactions and leading to a further reduction in the total free energy of the system. Micelle formation occurs above a specific equilibrium concentration, termed the critical micelle concentration (CMC). How the amphiphiles pack into the micelle, and hence the morphology formed, is related to the amphiphile shape which depends on the relative size of the hydrophobic and hydrophilic parts under equilibrium self-assembly conditions as this determines the curvature of the hydrophilic/hydrophobic interface. The packing preferences can be analysed in terms of the dimensionless "packing parameter" *P*, which is defined as:

$$P = \frac{v}{a_0 l_c}$$

where *v* is the volume of the hydrophobic hydrocarbon chain, a_0 is the area of the hydrophilic head group, and l_c is the length of the hydrophobic tail normal to the interface (Figure 1). Typically, spherical micelles are favoured for $P \leq 1/3$, cylindrical (also known as worm-like or rod-like) micelles for $1/3 \leq P \leq 1/2$, vesicles for $1/2 \leq P \leq 1$.[38, 39] It is noteworthy that this geometric approach makes a prediction of the equilibrium morphology, which is generally accessible with molecular amphiphiles on account of rapid exchange between the aggregated (micelle) and molecularly dissolved (unimer) state.

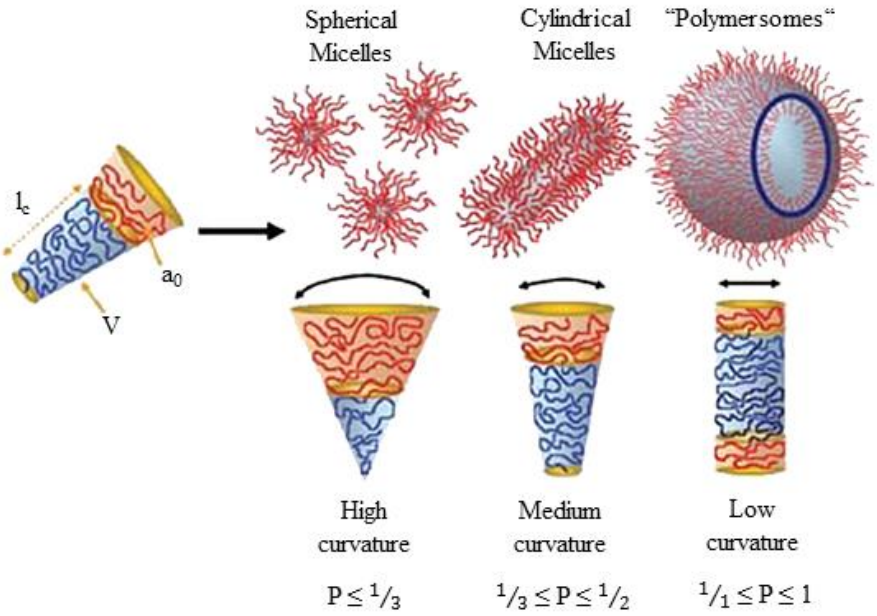

Figure 1. The thermodynamically-preferred morphology of the self-assembled BCPs in a selective solvent can be predicted by means of the dimensionless "packing parameter" *P*. Reproduced with permission from ref. [1] (copyright 2009 Wiley-VCH).

As with the case of molecular amphiphiles, BCPs can self-assemble into micelles with core-shell structures in selective solvents above the CMC. Morphologies, such as spheres, cylinders (or worms or rods), and vesicles, are also commonly observed (Figure 1).[2-6, 18, 40, 41] The micelle core is formed by the insoluble, solvophobic block(s) and the corona (or shell) by the soluble solvophilic block(s), which leads to colloidal stabilization of the micelle in solution.[3, 42-46] The role of entropy in self-assembly, however, is smaller (especially in non-aqueous solvents), as a result of the reduced translational freedom of macromolecules with respect to low molar mass species.[37] There is, nonetheless, an unfavourable entropic contribution from the stretching of the solvophobic chains within the micellar core. The reduction in interfacial energy between the core-forming block and the solvent, and the presence of repulsive interactions between the solvophilic coronal chains which cause stretching constitute additional opposing enthalpic and entropic contributions to the free energy of the system, respectively. In practice, the thermodynamically preferred micelle morphology often mainly depends on the volume fractions of the solvophobic and solvophilic

blocks, which are related to their molar masses and chemistries. Unlike the self-assembly of molecular amphiphiles in aqueous solution, however, the volume of solvophilic, and hence swollen, corona-forming block, and hence the effective value of a_0, depends significantly on the quality of the solvent mixture, thereby severely reducing the quantitative predictive ability of the packing parameter concept for BCPs.[39] Even more importantly, unless the concentration of common solvent is high, exchange of BCP molecules between micelles is often very slow relative to the assembly process, implying that thermodynamic equilibrium does not exist and that the resulting assemblies are formed under kinetic control.[40, 47] The packing parameter is therefore not useful to interpret the formation of many far-from-equilibrium BCP micelle morphologies and the major use for this concept is for qualitative predictions of, and understanding of transitions between, thermodynamically preferred assemblies.[1, 48]

Although BCP micelles are generally relatively robust and stable to solvent evaporation, in solution the stability is limited to the use of block selective solvents. Cross-linking of the micelle core[49] or corona[50-54] can "lock-in" the micelle structure and make it permanent.[55] This very useful and now well-developed method allows transfer to a common solvent that is good for both the core- and corona-forming blocks without dissociation or a change in morphology. The stability of the crosslinked micelles to shear forces is also dramatically enhanced.[54]

3. BCP Micelles with an Amorphous Core: From Morphological Simplicity to Complexity

3.1 Common morphologies

Compared to BCP self-assembly in the solid state, the solution self-assembly of BCPs is a more complex process because of the presence of segment interactions with the solvent as well as each other, making it more difficult to predict micelle morphologies and

morphological transitions theoretically.[18] Early work on BCP self-assembly followed on from the discovery of living anionic polymerizations and mainly focused on diBCPs with amorphous core-forming blocks and relatively long corona-forming segments. The reports mainly described the formation of "star-like" spherical micelles[3, 23, 56] and, much less commonly, non-spherical morphologies[57, 58] such as cylinders. In the mid 1990s a major development involved the seminal work of Eisenberg on BCPs with short corona-forming blocks and studies of the resulting "crew-cut" micelles.[59-61] Systematic studies permitted key insights into how various structural and experimental factors allow the resulting morphologies to be predicted and tuned.[1, 6, 18] For example, in the case of PS_{200}-*b*-PAA_x (PAA = poly(acrylic acid), PS = polystyrene) diBCP micelles in hydrophilic media (DMF-water solution), a change in the degree of polymerization (DP_n) of the PAA block resulted in a morphological change from "crew-cut" spheres with a PS core (x = 21), to cylinders (x = 15), to vesicles (x = 8), and finally to large compartment micelles (x = 4), attributed to decreased intercoronal chain repulsions and the consequential preference for a core-corona interface with lower mean curvature. This series of morphological changes is qualitatively in accordance to the predicted micelle morphology trends using the packing parameter concept (see Section 2).[61] Further parameters that influence the micelle morphology include the polymer concentration, solvent composition, and temperature. This is typically shown in phase diagrams in which the (assumed) equilibrium morphologies for a given BCP and temperature are illustrated as a function of block ratio, copolymer concentration, or solvent composition, separated by phase boundaries. The morphological phase diagram for a given PS-*b*-PAA diBCP in a dioxane-water solvent mixture revealed that pure spherical, cylindrical and vesicle phases, as well as a morphological mixture thereof can form depending on both the copolymer concentration and the water content.[45] Cylinders were observed in a restricted region of phase space bounded by coexistence regions with spherical or vesicle morphologies,[45] a feature typically found for BCP phase diagrams where the core-forming block of the BCP is amorphous.

3.2 Multicompartment nanoparticles from BCPs

Access to more complex micelle morphologies, such as multicompartment assemblies, has attracted significant recent attention and this has been partly motivated by analogies with cargo-carrying proteins and cells. Their preparation can be achieved by tuning segment-solvent interactions as well as the miscibility of constituent coblocks (e.g. the incompatibility between fluorinated and non-fluorinated blocks), and by triggering the BCP self-assembly by means of external stimuli (e.g. through electrostatic interactions). Compartmentalization can be induced either in the micelle core or corona via the solution self-assembly of diBCPs through the use of non-covalent interactions involving blends, and also, more generally, by the use triBCPs. In the remainder of this section, we give an overview of the preparation of multicompartmental nanostructures, showing conceptually different approaches to the solution self-assembly of BCPs. For detailed reviews on the subject of multicompartmental BCP-based nanostructures, the reader is referred to the literature.[13, 62-66] It should be noted that the use of crystallizable, core-forming blocks also provides an alternate route to multicompartmental micelles (see section 4.3).

The aqueous self-assembly of a mixed-arm star triblock terpolymer with three mutually immiscible blocks, poly(ethylene oxide) (PEO), poly(ethyl ethylene) (PEE), and poly(perfluoropropylene oxide) (PFPO) provides an informative example. The star rather linear structure suppresses the formation of core-shell-corona structures as all three domains must meet at a common junction. The two hydrophobic, but immiscible, PEO and PFPO blocks form the micelle core but remain in contact with the hydrophilic, corona-forming PEO block. Depending on the relative block lengths, the interfacial energies between the block segments as well as between the block segments and the solvent molecules (water) can be altered and thus, the micelle structure can be varied, for example, from discrete multicompartment micelles to worm-like micelles with segmented cores.[67, 68]

In another approach, droplet-confined self-assembly was reported for PS-*b*-P2VP (P2VP = poly(2-vinylpyridine)) and PS-*b*-P4VP (P4VP = poly(4-vinylpyridine)) diBCPs.[69, 70] A PS-*b*-P2VP emulsion was obtained by adding water containing the amphiphilic cationic surfactant cetyltrimethylammonium bromide (CTAB) to a PS-*b*-P2VP solution in chloroform, followed by ultrasonication. By evaporating the $CHCl_3$ in the emulsion droplets, the BCP concentration increased and microphase separation occurred, leading to surfactant-coated BCP particles with a lamellar structure. The interfacial energy between the aliphatic tail of the surfactant CTAB and PS chains is lower compared to the corresponding energy with P2VP chains, leading to a preferred adsorption of CTAB on PS. This led to a radial lamellar morphology with the PS layer adjacent to the CTAB layer, which forms the shell of the emulsion droplet (see Figure 2a). The preferred adsorption of CTAB on PS can be prevented by the addition gold nanoparticles, coated thiol-terminated poly(styrene-b-1,2- and 3,4-isoprene) ligands, to a PS-*b*-P2VP solution in chloroform. This led to a morphological change from spherical, radial lamella to axially stacked lamella after emulsification and evaporation of the $CHCl_3$ phase (see Figure 2b).[69]

Particles with a stacked lamellar morphology composed of PS-*b*-P4VP, also prepared by emulsion droplet confined self-assembly, were used to create Janus nanodiscs (see Figure 2c). By selective disassembly of P4VP layers in ethanol at 30 °C via sonication, the stacked lamellar structures were deconstructed into P4VP/PS/P4VP nanodiscs. CTAB was used to occupy the PS intermediate layer edge and so prevent an enveloping of the intermediate PS layer by adjacent P4VP chains. The P4VP layers were cross-linked with 1,5-diiodopentane in ethanol and, upon subsequent diffusion of chloroform, the cross-linked sandwiched nanodiscs separated into individual Janus nanodiscs.[70]

Liquid crystalline rod-coil diBCPs have been used to fabricate spherical, cylindrical and vesicle micellar morphologies that exhibit internal compartmentalization due to the mesogenic block.[71-73] For example, the solution self-assembly of PEO-*b*-PB diBCPs, which were functionalized with mesogens via thiol-ene chemistry, was found to afford vesicles with smectic stripes.[72]

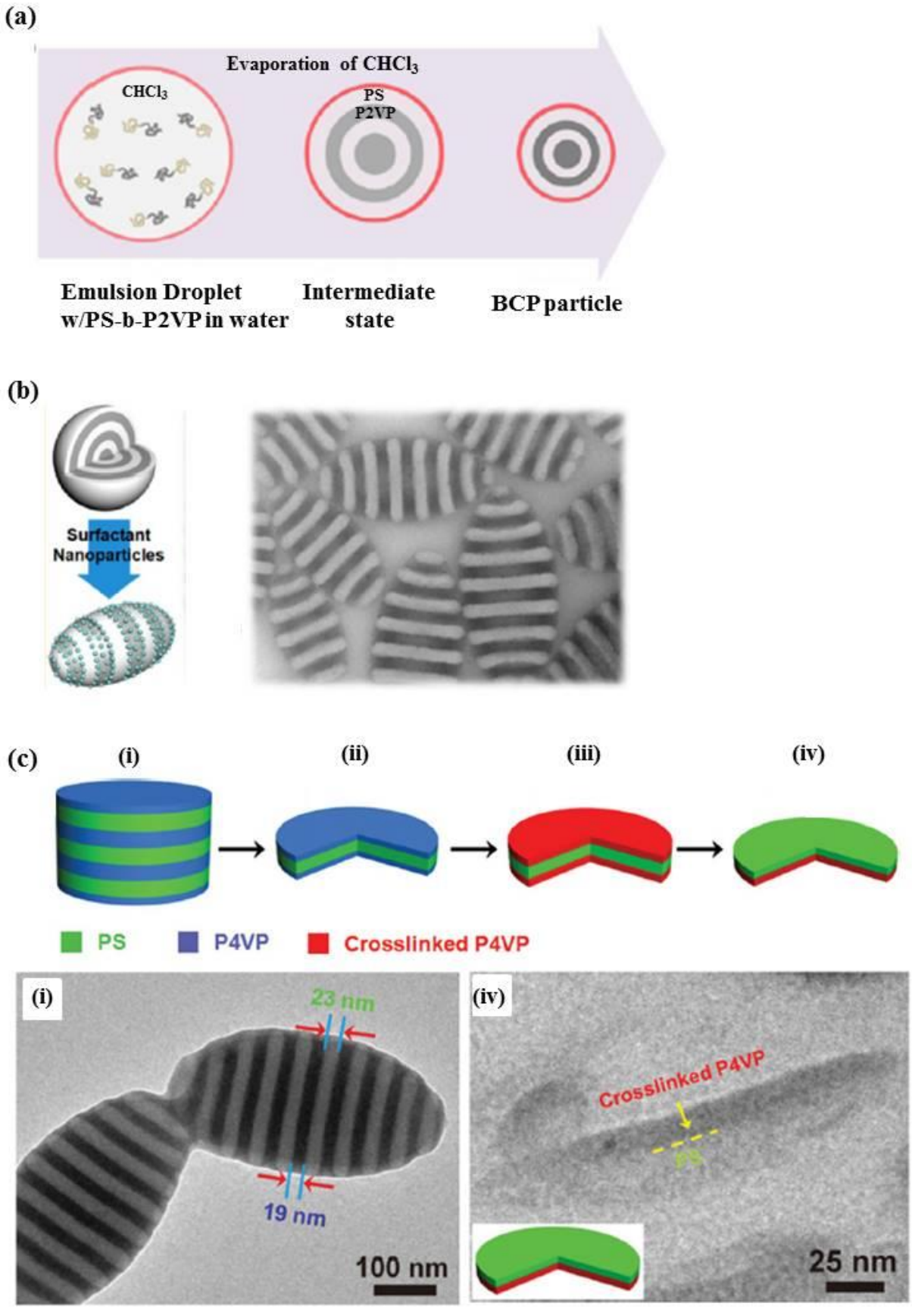

Figure 2. Emulsion droplet confined self-assembly of diBCPs. (a) Schematic representation of the self-assembly process of PS-b-P2VP in a chloroform-in-water emulsion droplet, induced by the evaporation of chloroform. (b) Schematic representation of the change in the morphology and shape of

PS-*b*-P2VP micelles. This change was found to be due to the presence of surfactant nanoparticles. The TEM image shows the resulting axially stacked lamellar morphology. (b) Schematic representation of the synthesis of Janus nanodiscs from stacked PS-*b*-P4VP lamellae obtained via droplet confined self-assembly. TEM image of the initial PS-*b*-P4VP stacked lamellae (step i) and the final Janus nanodiscs (step iv). (a,b) Reproduced with permission from ref. [69] (copyright 2013 American Chemical Society) and (c) reproduced with permission from ref. [70] (copyright 2014 WILEY-VCH).

The compartmentalization of the micellar core or corona can be achieved by non-covalent supramolecular interactions within a blend of diBCPs. This approach involves the confinement of immiscible BCP phases, for example via short-range attractive, electrostatic forces. Blending PB-*b*-PEO and PB-*b*-PAA diBCPs in aqueous solution led to the formation of vesicles composed of a mixed PEO/PAA corona. The divalent cations Ca^{2+} and Cu^{2+} were then able to cross-bridge amphiphilic polyanions, and the formation of PAA/Ca^{2+} and PAA/Cu^{2+} complexes induced gelation. This led to phase -separation of the corona-forming blocks (PAA and PEO) and the formation of circular domains, which coarsen in order to reduce the interfacial energy. The domain sizes change with the blend ratio of PB-*b*-PAA and PB-*b*-PEO, resulting in Janus vesicles for a ratio of 1:1, and inverse domains for a ratio of 3:1 (see Figure 3). At high pH values, PAA exhibits a negative charge and this resulted in the formation of phase-separated, segmented cylindrical micelles.[74]

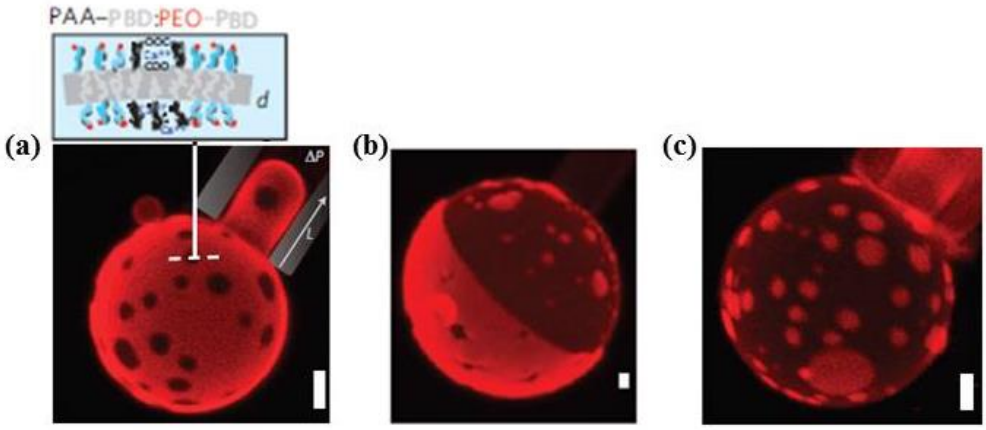

Figure 3. Confocal microscopy images revealing the microphase separation of PB-*b*-PEO and PB-*b*-PAA in aqueous solution due to gelation of PAA with divalent cations. Depending on the blend ratio of PB-*b*-PAA and PB-*b*-PEO, different micellar morphologies were observed (a-c). Scale bars: 2 µm. Reproduced with permission from ref. [74] (copyright 2009 Nature Publishing group).

Compartmentalization of the micelle corona has also been achieved through interpolyelectrolyte complexation (see Figure 4a).[75-79] Spherical multicompartment micelles were formed from the self-assembly of polybutadiene-*b*-poly(1-methyl-2-vinylpyridinium)-*b*-poly-(methacrylic acid) (PB-*b*-PVq-*b*-PMAA) linear triblock terpolymers in aqueous solution. These micelles were composed of a hydrophobic PB core, intramicellar polyelectrolyte complex (im-IPEC) patches of PVq/PMAA on the core surface, and a negatively charged corona of excess PMAA. All-hydrophilic cationic diBCPs, such as poly(L-lysine)-*b*-PEO, can coordinate to PB-*b*-PVq-*b*-PMAA. This led to the formation of ionically grafted PMAA, and finally, when anionic and cationic charges were neutralized, the IPECs phase-separated from the aqueous solution and ordered IPEC segments within the micelle corona formed. Due to the high number of polymeric chains and the dense packing of the non-ionic blocks, the corona-forming chains were stretched, leading to anisotropic IPEC morphologies. Cylindrical and lamellar IPEC morphologies were obtained depending on the block ratio of the solvent-swollen PEO micelle corona and the hydrophobic IPEC (Figure 4b and c).[75]

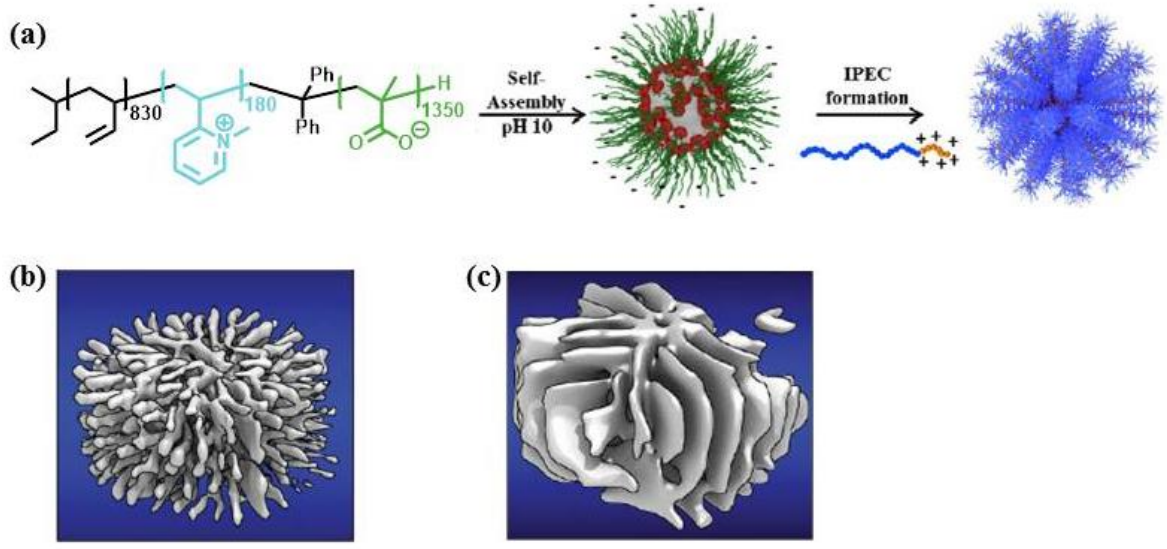

Figure 4. (a) Formation of corona-compartmentalized micelles via interpolyelectrolyte complexation. The triblock terpolymers PB-*b*-PVq-*b*-PMAA self-assemble in water to give multicompartment micelles exhibiting a PB core (gray), PVq/PMAA intramicellar IPEC domains (red), and excess PMAA corona (green). All-hydrophilic diBCPs added can complex PMAA, resulting in nanostructures with anisotropic IPEC morphologies. (b,c) Tomographic reconstructions of "sea-urchin" micelles with cylindrical IPEC morphologies (b) and "turbine" micelles with lamellar IPEC

morphologies (c). Reproduced with permission from ref.[75] (copyright 2014 American Chemical Society).

3.3 Two-step self-assembly strategies to form hierarchical micellar structures. The step-wise formation of multicompartment nanostructures involves the synthesis of precursor micelles, which are at thermodynamic equilibrium (or alternatively in a kinetically trapped state stable over a sufficiently long time), as the first step. These precursor micelles function as building blocks, which that can self-assemble into well-defined multicompartment structures in a subsequent step when triggered by external stimuli. Various external triggers can induce the second self-assembly process, such as solvent composition/nature of non-solvent,[80-82] temperature,[83] electrostatic interactions,[84, 85] metal-coordination,[86-88] pH,[89] hydrogen bonding,[90-92] and crystallization (see Section 4).

Sequential addition of non-solvents has been shown to induce the formation of remarkable hierarchical structures from PS-*b*-PB-*b*-PMMA and PS-*b*-PD-*b*-PMMA (PMMA = poly(methyl methacrylate), PD = poly(3-butenyl(dodecyl)sulfane) triBCP precursor micelles (see Figure 5).[80, 81] When dispersed in a non-solvent for the PB or PD blocks, the triBCPs PS-*b*-PB-*b*-PMMA and PS-*b*-PD-*b*-PMMA self-assembled into monovalent Janus micelles and divalent, linearly aggregating micelles, respectively (see Figure 5, hierarchical level 1). A selective solvent for the PMMA blocks was then introduced to both solutions, resulting in a collapse of the PS blocks, followed by micelle aggregation. PS-*b*-PB-*b*-PMMA formed spherical clusters while PS-*b*-PD-*b*-PMMA self-assembled into linear supracolloidal polymer chains (see Figure 5, hierarchical level 2). If both micelle morphologies are mixed before introducing the selective solvent for the PMMA blocks, the formation of a mixed superstructure was observed (see Figure 5, hierarchical level 2). In these superstructures, the PS-*b*-PB-*b*-PMMA micelles were situated on the PS segments of the linear, core-segmented PS-*b*-PD-PMMA cylinders.[81]

By introducing a combination of electrostatic forces and a non-solvent, core-compartmentalized micellar structures were obtained. When PS-*b*-PMA-*b*-PAA (PMA = poly(methyl acrylate)) was self-assembled in a THF/water mixture into this led to the anticipated micelles with a PS core, a PMA shell, and a PAA corona. In the presence of organic diamines, and increasing amounts of water to increase the polarity of the solvent mixture, complexation of PAA by the diamine occurred while the hydrophobic PMA and PS blocks aggregated. Consequently, striped cylinders with alternating hydrophilic and hydrophobic layers were formed.[84] On starting at a relatively high water content, PS-*b*-PMA-*b*-PAA formed spherical micelles. Upon addition of THF, a morphological transition from spheres to discs was observed. Finally, at a high THF/water ratio, the disk-like micelles stacked via their PAA/diamine faces through attractive electrostatic interactions, leading to one-dimensional packed structures.[84] Approaches using crosslinkable precursors that yield segmented cylinders have also been reported.[93]

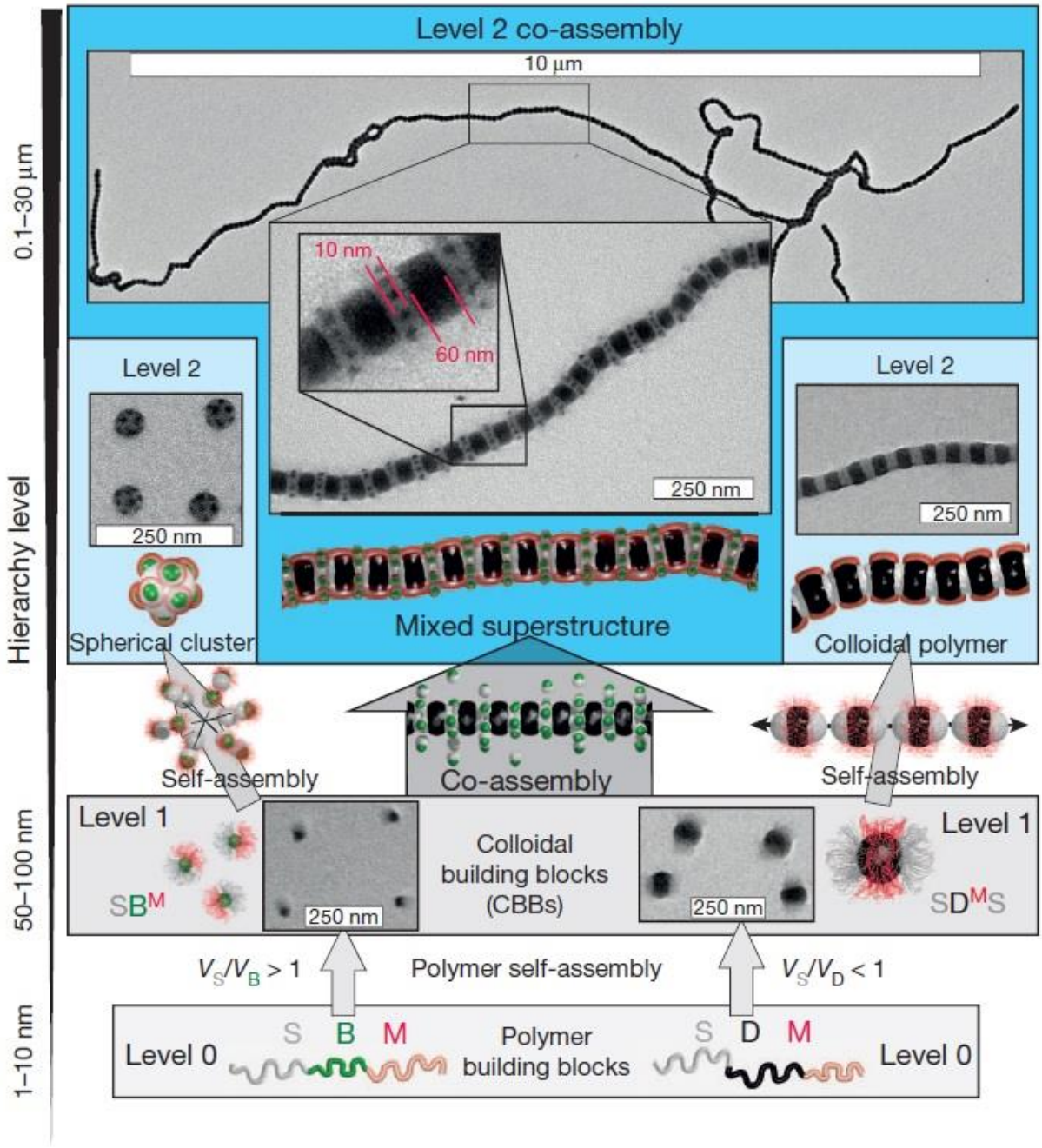

Figure 5. Stepwise assembly of PS-*b*-PB-*b*-PMMA (SBM) and PS-*b*-PD-*b*-PMMA (SDM) triBCPs into hierarchical micellar structures, induced by changes in the solvent composition. Depending on the volume ratios of the core-forming blocks, monovalent SB^M and divalent SD^MS colloidal building blocks formed by polymer self-assembly (level 1). These building block can self-assemble into spherical clusters or linear supracolloidal chains or co-assemble into a mixed superstructure (level 2). Reproduced with permission from ref. [81] (copyright 2013 Nature Publishing group).

4. BCP Micelles with Crystalline Cores: Non-spherical Morphologies with Dimensional Control

4.1 Influence of crystallization on self-assembled BCP morphologies

Although early work on BCP self-assembly was dominated by studies of materials with amorphous core-forming blocks, several reports as early as the mid 1960s described the formation of platelet micelles with a crystalline PEO core from the diBCP PEO-b-PS in selective solvents for PS.[94, 95] Further studies of similar materials were described in the early to mid 1990s[96, 97] together with a theoretical analysis and development of scaling relationships[98] for micelles with crystalline cores. Since the late 1990s a wide variety of BCPs with crystallizable core-forming blocks have been studied.[99, 100]

A distinct and advantageous feature to emerge from this work is the preference for the formation of non-spherical morphologies such as cylinders/fibers and platelets that are, in general, challenging to access, especially in pure form, from the self-assembly of BCPs with amorphous cores over a substantial region of phase space. This has led to the introduction of the term "crystallization-driven self-assembly" (CDSA) for the formation of BCP micelles where crystallization plays a key role in the determination of the micelle morphology. For example, studies of BCPs with the metal-containing polymer poly(ferrocenyldimethylsilane)[101] (PFDMS) as the crystallizable core-forming block revealed the formation of cylindrical/fiber-like micelles when the poly(dimethylsiloxane) (PDMS) corona-forming block was much longer (block ratio PFDMS:PDMS 1:6). On the other hand, self-assembly above the melting temperature of PFDMS followed by rapid quenching to prevent crystallization of the PFDMS core gave spherical micelles which would be the expected morphology simply based on the block ratio.[102] Moreover, studies of PFDMS BCPs with short corona -forming blocks showed that these materials yielded platelet micelles.[103]

A wide range of crystallizable core-forming blocks other than PFDMS have now been employed to enable the formation of cylindrical/fiber-like micelles with crystalline cores and these include poly(3-hexylthiophene)),[104-109] poly(L-lactic acid) (PLLA),[110-113] polycaprolactone (PCL),[114, 115] PEO,[116] PE,[117-120] poly(acrylonitrile),[121] poly(ferrocenyldimethylgermane) (PFDMG),[122] poly(ferrocenyldiethylsilane) (PFDES),[123] poly(ferrocenylmethylsilane)(PFMS),[124] PCL/PLLA,[125] poly(perfluoroethyloctyl-methacrylate),[126, 127] cholestorol-based polymers,[128] polyacetylene,[129, 130] poly(*p*-phenylene),[131] poly(3-heptylselenophene),[132] polyfluorene,[133-135] poly(*p*-phenyleneethynylene),[136, 137] poly(*p*-phenylenevinylene),[138-142] cyclic polypeptoids,[143] and poly(2-isopropyl-2-oxazoline).[144]

The relationship between core crystallinity and the observed morphology appears to related to variations of a range of parameters, including core/coronal block ratios,[145] temperature,[102] and solvent conditions.[146] As cylinders/fibers possess an intermediate mean curvature compared to platelets and spheres it might be expected that the resulting morphology in this case reflects a free energy counterbalance arising from contributions due to crystallization, which favours zero curvature of the core-corona interface,[48] and intercoronal chain repulsions, which promote maximum curvature. The formation of platelets in preference to vesicles can be explained by the rigidity arising from crystalline core, which presumably hinders the closure necessary for the formation of the curved interface from a bilayer. Nevertheless, the overall relationship between core crystallization and morphology appears to be complex and further studies and insight are needed. For example, studies of PFDMS-b-P2VP (P2VP = poly(2-vinylpyridine), block ratio 1 : 6) in solvents selective for P2VP can yield either cylinders/fibers or platelets with crystalline PFDMS cores depending on the amount of common solvent added to the medium. Presumably the presence of common solvent facilitates more extensive crystallization of the core-forming block.[147] Moreover, spherical

micelles with crystalline cores have been reported with other BCP systems. For example, the dissolution of the triBCP PS-*b*-PE-*b*-PMMA with a crystalline PE core-forming central block has been studied under several different solvent conditions.[146] In a moderately poor solvent for the PE core, cylindrical micelles were obtained, due to a crystallisation of the PE block. When self-assembly was carried out in a very poor solvent for PE, spherical micelle formation was followed by confined PE crystallisation. This resulted in spheres with a core with an apparent cubic appearance.[146] In another fascinating study, it has been shown that homochiral PLLA-*b*-PAA (PLLA = poly(*L*-lactic acid),) and PDLA-*b*-PAA (PDLA = poly(*D*-lactic acid)) BCPs independently form cylinders with crystalline cores in THF/H_2O at 65°C. However, on heating a 1:1 mixture of both BCPs in solution or a mixture of the respective cylinders under the same conditions, spherical micelles with a crystalline stereocomplexated PLA core were formed (Figure 6) by an apparent unimer exchange process.[148] These examples underscore the fact that for BCP micelles with crystalline cores, the packing parameter is of very limited predictive utility for the rationalisation of observed morphologies.

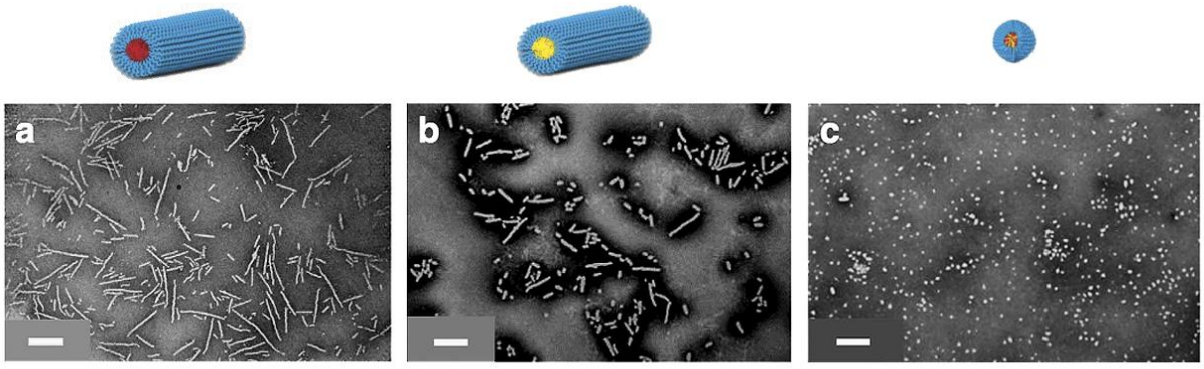

Figure 6. Scheme depicting the formation of crystalline spherical micelles by stereocomplexation of cylinder-forming pure isotactic PLLA-*b*-PTHPA and PDLA-*b*-PTHPA. Below the scheme: TEM images of drop-cast micelles stained with uranyl acetate. (a) and (b) depict cylindrical micelles formed by pure isotactic PLLA-*b*-PTHPA and PDLA-*b*-PTHPA, respectively. TEM image (c) depicts the spheres formed through stereocomplexation of the two stereoisomers. Scale bars= 500 nm. Reproduced with permission from ref. [148] (copyright 2014 Nature Publishing Group).

4.2 Dimensional control: "Living" Crystallization-Driven Self-Assembly

Cylinders/fibers or platelets formed by the dissolution of BCPs with a crystallizable core-forming block in a selective solvent possess a broad length or area distribution, respectively. This is a likely consequence of the random and slow nature of the homogeneous nucleation (or self-nucleation) process, which is believed to be a prerequisite for micelle formation under many conditions where self-assembly does not precede crystallization. In 2007 it was found that elongation of pre-existing cylindrical/fiber-like micelles with a crystalline PFDMS core occurs in solution upon further addition of unimer.[149] This surprising result was attributed to the exposed crystalline faces at each micelle core terminus being available for subsequent polymer crystallisation via an epitaxial growth process.[147, 150] Ultrasonication of cylinders formed by self-nucleation can lead to very small "seed" micelles that can be used as "initiators" for subsequent growth of micelles featuring very low length polydispersities (Figure 7).[151] Under these "seeded growth" conditions the aforementioned problems associated with the slow formation of crystal nuclei via homogeneous nucleation are circumvented and the increase in length of cylindrical micelles is linearly dependent on the ratio of the amount of unimer added to that of the seeds. This process can be considered analogous to a living covalent polymerisation and it has been termed "living" CDSA (Figure 7). Using this "seeded growth" living CDSA process low dispersity cylindrical micelles with lengths from tens of nanometers to several micrometers can be produced (Figure 8).[151] Similar living CDSA processes have been reported for other BCPSs such a PS-*b*-PE-*b*-PS triblock terpolymer with a crystallisable central PE block to yield uniform cylinders/fibers of controlled length up to 500 nm.[117] Fibers of P3HT-*b*-PDMS (of length up to 250 nm)[104] and P3HT-*b*-P2VP (up to 300 nm) with a π-conjugated have also been prepared.[105]

An alternative living CDSA route to monodisperse cylinders with PFDMS cores in solution is via "self-seeding" (Figure 7, top). To facilitate the process this involves the mild sonication of polydisperse cylindrical micelles to form shorter micelles that are longer and of higher length polydispersity than those used for "seeded" growth. Thermal annealing at a constant temperature (typically between 55°C and 75°C) then results in dissolution of the smaller crystallites, as these exhibit a lower T_m (Figure 7, below).[152] The unimers released are then free to crystallize upon the surviving, highly crystalline micelles on cooling, producing relatively monodisperse cylindrical micelles. The selected temperature and sample thermal history have an effect on the length of fibres that are obtained through this method and the presence of common solvent can be used in a manner than is equivalent to the use of temperature.[153] For example, cylinders of controlled length have been obtained through self-seeding methods for a range of BCPs including P3HT-*b*-PS,[106] and PFDMS-*b*-PDMS.[153] Normally cylindrical seeds possess two exposed termini for subsequent addition of unimer but seeds with undergo unidirectional growth from one terminus have also been prepared.[154] The samples of monodisperse cylinders prepared via living CDSA methods appear indefinitely stable in selective solvents at room temperature due to kinetic trapping: the CMC is effectively zero.[63, 153]

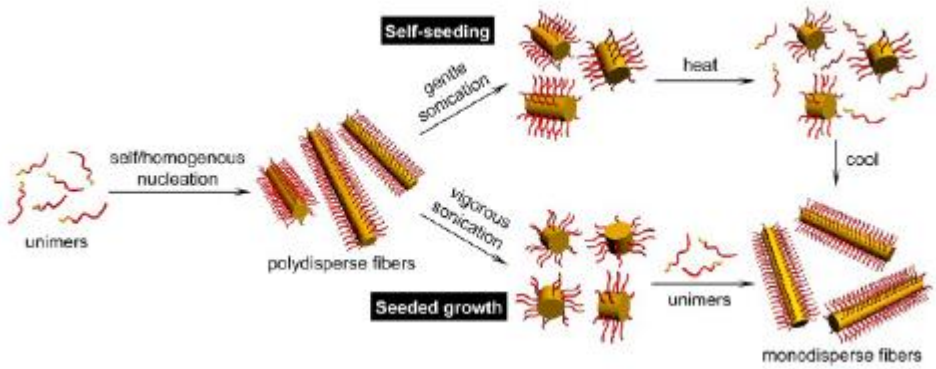

Figure 7. Methods for producing monodisperse cylindrical micelles with crystalline cores in solution via "self-seeding" (upper route) and "seeded growth" (bottom route). Reproduced with permission from ref [155] (copyright 2015 American Chemical Society).

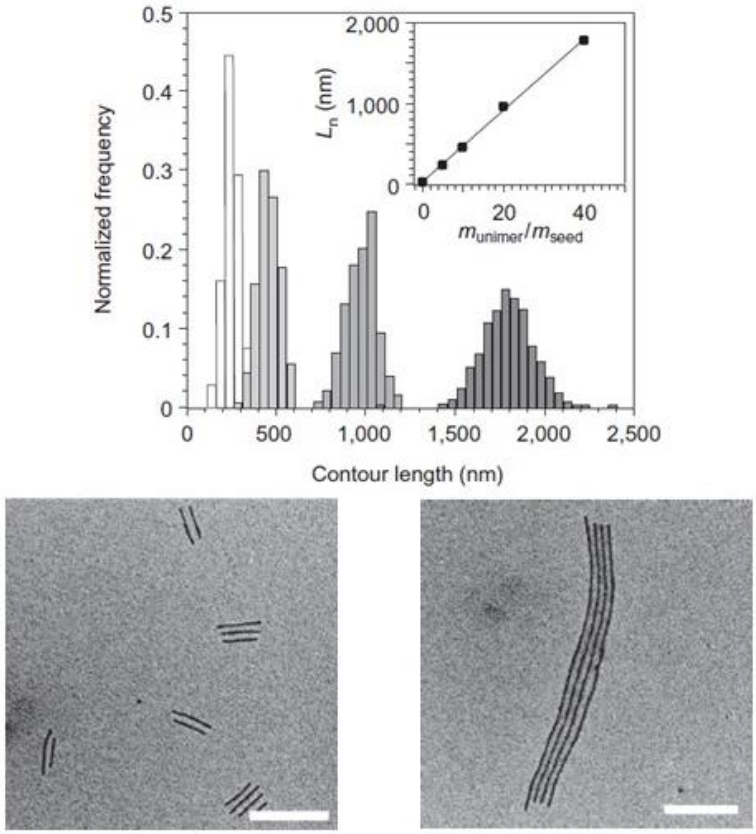

Figure 8. Histograms of the contour length distribution of monodisperse cylindrical micelles, obtained by seeded-growth, in which the inset graph displays the linear dependence of micelle contour length on the unimer-to-seed ratio. To the right, displays two samples after addition of 250 μg (top) and 2000 μg (bottom) PI_{550}-*b*-$PFDMS_{50}$ as 10 $mgmL^{-1}$ solutions to PFDMS-*b*-PDMS crystallites in *n*-hexane. Scale bars= 500 nm Reproduced with permission from Ref.[151] (Copyright 2010 Nature Publishing Group).

4.3 Block and patchy comicelles using "Living" CDSA

Addition of a BCP with a different corona-forming block to that for the seed micelles results in the growth of segmented multi-block comicelles.[149] It is therefore possible to produce segments of desired length with spatially located coronal chemistries along the length of the block comicelle. For example, block comicelles with hydrophobic and hydrophilic regions of controlled length or hydrogen-bonding capabilities were prepared through the sequential addition of PFDMS BCPs with appropriate coronal functionalization to cylindrical micelle seeds.[156-158] Centrosymmetric and non-centrosymmeric block comicelles can be prepared depending on the nature of the seed.[154] Examples are not limited to block comicelles formed by PFDMS BCPs and include cylinders with crystalline PE cores and patch-like terminal

coronal segments of PS and PMMA[146] from the addition of PS-*b*-PE-*b*-PMMA triblock terpolymer to PS-*b*-PE-*b*-PS seeds (Figure 9a).[117] Analogous behavior was observed in the case of seeded growth of miktoarm PI-*b*-PS-*b*-PFDMS star terpolymers in solution.[159] Triblock comicelles have also been prepared with a P3HT core.[106] "Bar-code" micelles with a PFDMS-core with corona blocks of different fluorescent color have also been reported (Figure 9b) as have gradient cylinders prepared by the simultaneous seeded growth of PFDMS BCPs that exhibit different rates of addition.[160] These multiblock micelles show no change after 1 year in solution, the lack of scrambling testifying to their kinetically-trapped, non-equilibrium nature in selective solvents under ambient temperature conditions.[63]

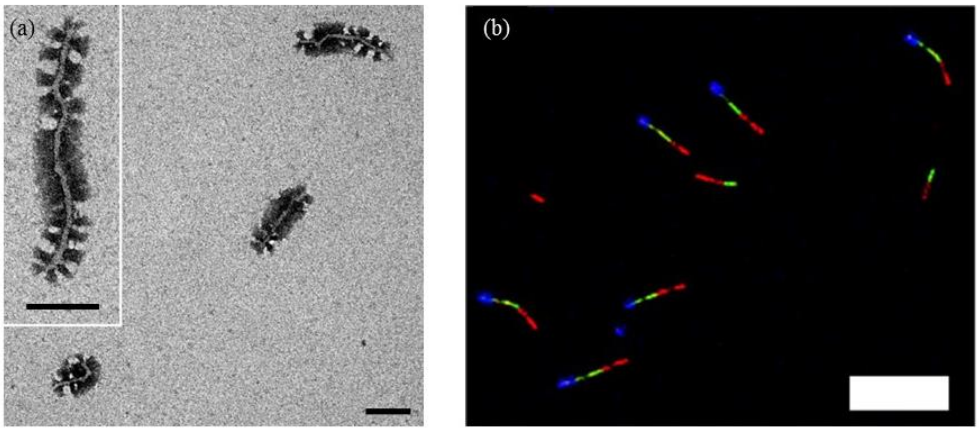

Figure 9. (a) TEM images of centrosymmetric triblock comicelles with patchy segments of controlled length, formed through seeded growth of PS-*b*-PE-*b*-PMMA unimer from PS-*b*-PE-*b*-PS micelle seeds. Scale bars = 100 nm. Reproduced with permission from ref.[117] (Copyright 2012 American Chemical Society) (b) LSCM micrographs of non-centrosymmetric block comicelles, formed by sequential addition of PFDMS-*b*-PDMS functionalised with various BODIPY dyes. Scale bar= 10 μm. Reproduced with permission from ref. [161] (Copyright 2014 Nature Publishing Group).

Block comicelles with a PFDMS core have also been prepared in aqueous media.[162] An amphiphilic linear-brush BCP, PFDMS-*b*-PAGE, decorated with triethylene glycol (TEG) (PFDMS-*b*-PEO-*g*-TEG), was prepared and self-assembled in DMF to form cylindrical micelles. Addition of PFDMS-*b*-P2VP to PFDMS-*b*-(PEO-*g*-TEG) micelles in isopropanol yielded B-A-B triblock comicelles. Subsequent quaternisation of the P2VP with dimethyl sulphate yielded stable BAB micelles of controlled dimension in aqueous solution via dialysis

from isopropanol into water. Potential use of these structures for DNA delivery was displayed by DNA complexation to the positively charged terminal segments. Linkage of cylindrical micelles by the DNA was observed, forming tethered block comicelle superstructures.[162]

Heteroepitaxial growth, involving the sequential crystallisation of two different core-forming polymers is potentially possible providing the lattice matching is sufficient (usually within 15%) and the rates of crystallization are compatible.[163] This has been achieved for the case of the addition of PFDMG-b-PI to PFDMS-*b*-PDMS seeds to yield a block comicelle with a crystalline junction between the PFDMG and PFDMS cores,[122] but has been unsuccessful in certain other cases.[123]

4.4 "Living" CDSA in 2D

Although the formation of 2D platelets is common for BCPs with crystallisable core-forming blocks,[94-97, 103, 164-171] the ability to control the size has remained a challenge. It is also possible to produce uniform 2D platelets of controlled dimensions by living CDSA.[145] Addition of PFDMS-*b*-PMVS (PMVS = poly(methylvinylsiloxane)), with a block ratio of 1:1, to cylindrical PFDMS-*b*-PDMS seeds formed colloidally stable lenticular platelets of up to 1 μm in length (Figure 10a). Two-dimensional living CDSA was confirmed as platelet areas were linearly dependent on the seed:unimer ratio. The sequential addition of unimers to lenticular platelets allowed for the formation of platelet block comicelles. Spatially defined regions were observed by imaging of BODIPY dye-functionalised PFDMS-*b*-PMVS separated by non-fluorescent PFDMS-*b*-PDMS spacers, through laser confocal microscopy.[145]

PFDMS BCP/homopolymer blends have been used to form rectangular platelets of controlled size through living CDSA, seeded by cylindrical PFDMS BCP micelles (Figure 10b).[172] PFDMS homopolymer/BCP blends consisting of a 1:1 w/w ratio in THF, subsequent addition

to a solution of seeds in a block selective solvent yielded uniform platelets with controlled dimensions. Platelet aspect ratios were dependent upon solvent conditions and the width of the cylindrical seeds used to nucleate growth.[172] The mechanism of seeded growth appears to be different to that of previously reported lenticular platelets, as growth occurred rapidly around the entire cylindrical seed, rather than initially at the exposed seed termini. The range of different coronal chemistries available for the formation of platelets by this method allowed for crosslinking of spatially specific regions. Addition of a good solvent to the platelets in solution dissolved uncrosslinked regions, forming 2D hollow structures of controlled size. Figure 10 displays the two principal methods for the formation of 2D structures of controlled dimension by "seeded" growth. It is also noteworthy that rectangular platelets have also been prepared from the seeded growth of more complex crystallisable building blocks, for example hyperbranched poly(ether amine) capped with polyhedral oligomeric silsesquioxane (POSS) groups.[173]

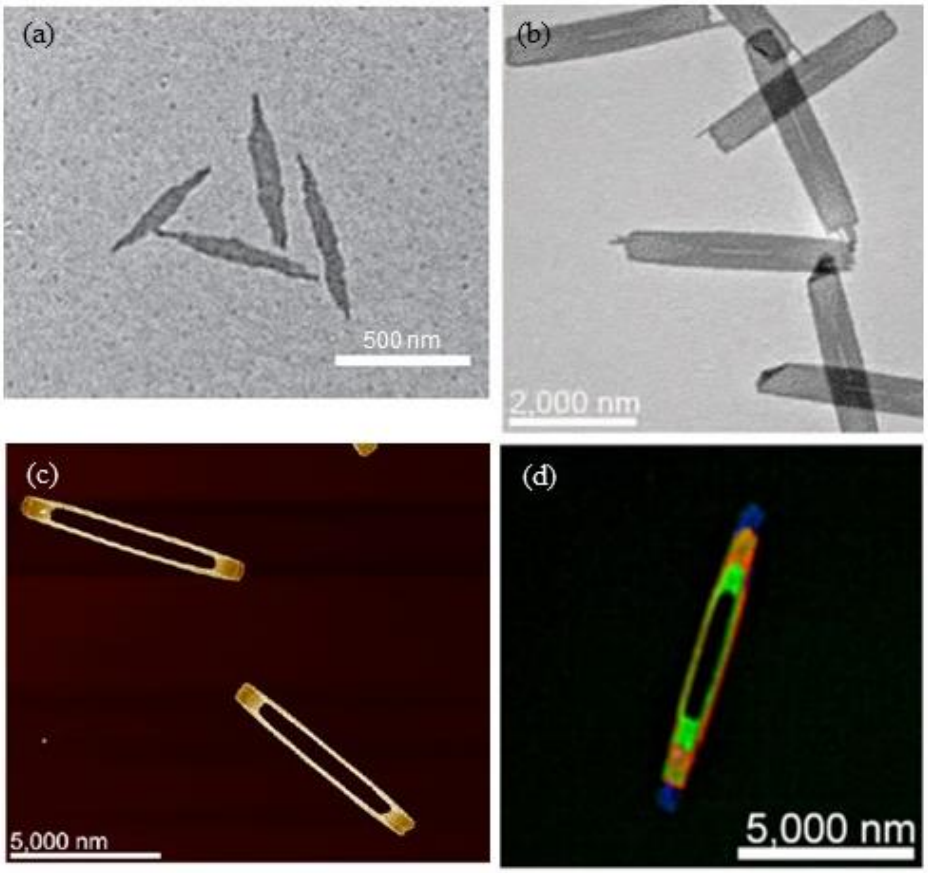

Figure 10. (a) TEM image of monodisperse lenticular platelets formed through the seeded growth of 1.3:1 $PFDMS_{114}$-*b*-$PDMS_{81}$ from cylindrical $PFDMS_{28}$-*b*-$PDMS_{560}$ 1:6 seeds in hexane. Reproduced with permission from ref. [145] (Copyright 2014 Nature Publishing Group). (b) TEM image of uniform rectangular platelets in solution from the seeded growth of a BCP/Homopolymer blend of $PFDMS_{36}$-*b*-$P2VP_{502}$/PFS_{20} 1:1 w/w ratio in a hexane/iPrOH solvent mixture of 1:3 v/v at 45 °C from $PFDMS_{28}$-*b*-$PDMS_{560}$ cylindrical micelles. (c) AFM image of hollow rectangular micelle structures, obtained through the selective cross-linking of P2VP-functionalised concentric platelet segments, followed by dissolution of the central uncross-linked segment in THF. (d) Structured illumination microscopy image of a RGB platelet comicelle, formed through the sequential addition of different dye-functionalised PFDMS BCPs/homopolymer blends. Reproduced with permission from ref. [172] (Copyright 2016 The American Association for the Advancement of Science)

4.5 Complex Micelle Architectures using Living CDSA

Living CDSA provides a route to a wide variety of more complex block architectures. The first examples involved cylinder-on-platelet structures known "scarf" micelles, which were prepared via the seeded growth of cylinder forming BCPs from seeds with a platelet morphology. For example, PFDMS-*b*-PI with a block ratio of 1:1 was observed to form platelets in xylene/decane solvent mixture.[122] Fragmentation by the sonication, followed by addition of cylinder-forming PFDMS-*b*-PI in THF/hexane mixture resulted in seeded growth

of cylindrical micelles to generate the "scarf" micelles. Hollow structures have been formed by the addition of cylinder-forming PFDMS-*b*-PI (block ratio of 1:6) to PFDMS-*b*-PDMS platelets. Addition of PFDMS-*b*-PI BCP also occurred around the edges of the platelet in addition to the ends. Crosslinking of the PI coronae resulted in a PFDMS-*b*-PDMS plate core with a cross-linked PFDMS-*b*-PI frame, so that subsequent dissolution of the central platelet in THF yielded hollow-"scarf" micelles.[174]

Other examples of complex micelle architectures accessible through living CDSA include multi-arm micelles, via the seeded growth of PFDMS BCP cylindrical micelles by homopolymer nanoparticles,[175] and hierarchical hybrid mesostructures obtained via the growth of PFDMS-*b*-P2VP micelles from silica nanoparticles and carbon nanotubes.[176, 177] "Branched" micelles can also be prepared by initiating the growth of $PFDMS_{21}$-*b*-PI_{132} unimer using $PFDMS_{133}$-*b*-PI_{1250} cylindrical seeds. Due to the difference in the respective degrees of polymerisation of the core-forming blocks, the growth of two or more cylindrical micelles could be initiated from the cylindrical seed termini.[155] Branching could also be achieved from PFDMS BCP cylindrical micelle seeds following the removal of a photocleavable corona.[178] PFDMS cylindrical BCPs have also been used as templates for sol-gel deposition to create coated nanowires (see section 6.3).[179,180]

As previously discussed, living CDSA provides a route to forming spatially segregated amphiphilic multi-block comicelles. Amphiphilic block comicelles consisting of a hydrophobic PFDMS-*b*-PDMS central segment with PFDMS-*b*-P2VP termini have been used to produce supermicelles through controlled aggregation.[156, 157] Dialysis of hydrophilic-hydrophobic-hydrophilic triblock comicelles from 3:1 isopropanol/hexane mixtures into pure isopropanol, resulted in the formation of supermicellar structures (e.g cylindrical supermicelles) driven by aggregation of hydrophobic cores.[156, 157] Through length

optimisation of the hydrophobic and hydrophilic sections, hierarchical assemblies of block comicelles were achieved such as cylindrical supermicelles.[157]

Hierarchical assemblies can also be achieved by using spatially-confined H-bonding between block comicelles.[181] Interactions between P2VP and OH-functionalised PMVS coronas have been utilised in the formation of large, supermicellar structures. Optimising the lengths of donor, acceptor and non-interacting comicelle segments allowed control over various hierarchical assemblies of block comicelles, including "windmill" and "cross" micelles (Figure 11).[182]

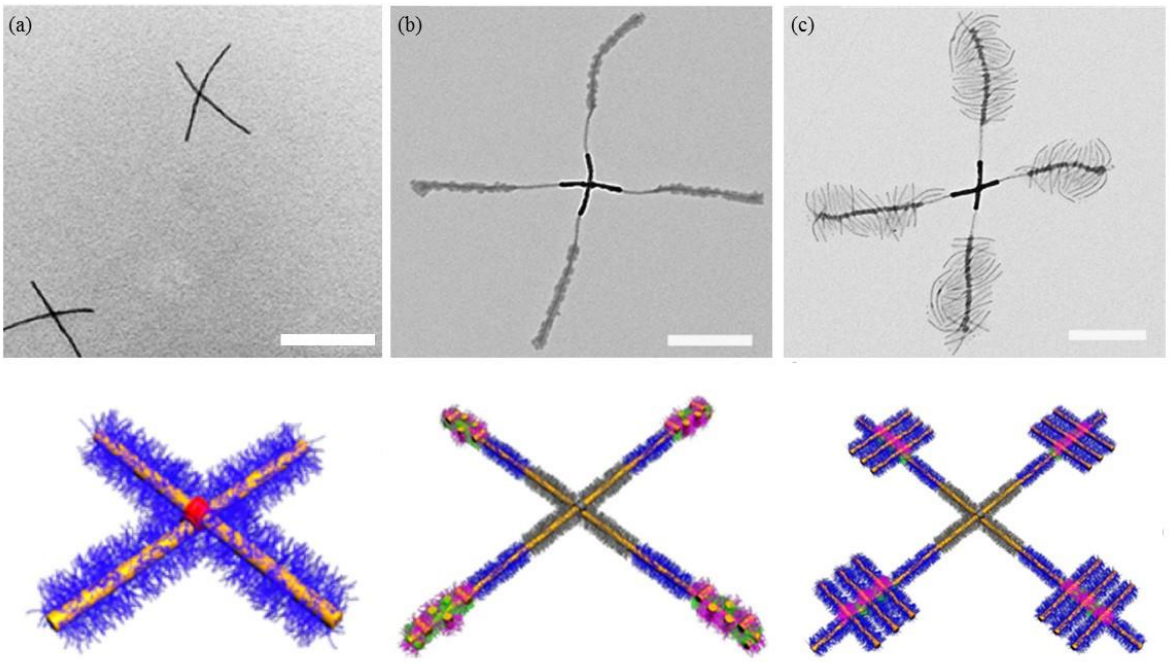

Figure 11. (a) TEM image of "cross" supermicelle structures, with a cartoon representation below, formed through solvophobic aggregation of 20 nm $PFDMS_{28}$-*b*-$PDMS_{560}$ micelle cores, depicted in red, with polar $PFDMS_{20}$-*b*-$PtBA_{280}$ end segments, depicted in blue, upon dialysis of the micelle solution from 1:4 hexane/isopropanol into MeOH. Scale bar = 500 nm. Reproduced with permission from ref. [183] (Copyright 2016 American Chemical Society) (b) TEM image of a "cross" supermicelle formed by stepwise hierarchical assembly, with a cartoon representation below. The micelle in iPrOH consists of a cross-linked "cross" central seed, non-interacting segments, depicted in blue, H_A segments depicted in green, decorated with H_D seeds, depicted in pink. Scale bar = 2 μm. (c) TEM image and cartoon representation of a "windmill"-like supermicelle structure formed from the addition of PFDMS-*b*-PtBA, depicted in blue, to the structure (b) in i-PrOH. Scale bar = 500 nm. (b,c) Reproduced with permission from ref. [181] (Copyright 2015 Nature Publishing Group).

5. Polymerization-induced self-assembly (PISA): Scaled Up Micelles

5.1 The challenge of scale-up.

Solution processing of BCPs is usually carried out in a post-polymerisation step that involves addition of a block selective solvent to a BCP, a protracted multistep process that leads to very low final BCP concentrations (< 1% solids by weight) that hinder commercial scale up. Polymerization-induced self-assembly (PISA) is the in-situ polymerization and solution self-assembly of amphiphilic BCPs and can be performed at high weight percent of solids (ca. 10 - 50% w/w solids) and therefore represents a scale-up process of potential industrial relevance. To date the majority of examples are based on dispersion polymerization or emulsion polymerization using controlled radical polymerization methods. Although the diBCPs used for PISA formulations can be synthesized by any living/controlled polymerization technique, most examples currently apply RAFT polymerization. In a typical PISA experiment, a macromolecular initiator is prepared, which will ultimately form the corona-forming "A" block of the BCP and functions as a soluble stabilizing block. In the second step, the macroinitiator is dispersed in the monomer and radical initiator in presence of a selective solvent. During the polymerization, the block length of the insoluble core-forming "B" block increases, inducing self-assembly of BCP micelles. Depending on the block ratio of the A and B blocks, different micellar morphologies have been obtained, including spheres, cylinders/worms, platelets and vesicles (Figure 12).[19, 20, 184]

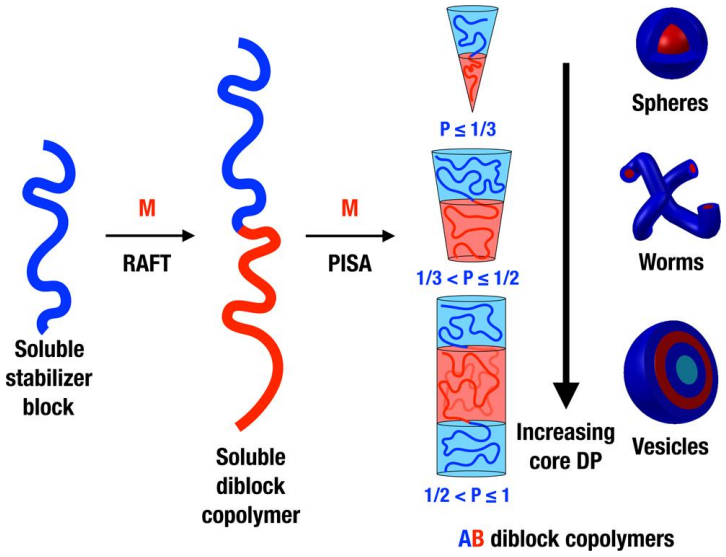

Figure 12. Synthesis of diBCP micelles by polymerization-induced self-assembly (PISA). Depending on the block ratio (i.e. degree of polymerization (DP) of core-forming vs. corona-forming blocks), different micellar morphologies can be accessed. Reproduced with permission from ref. [184] (copyright 2016 American Chemical Society).

PISA has emerged as an approach and has been carried out with a variety of functional monomers in a broad range of solvents, including polar solvents (such as lower alcohols),[19] non-polar solvents (such as *n*-alkanes, mineral oil, and poly(α-olefins)),[19] water,[20] and even supercritical carbon dioxide[185, 186] and ionic liquids.[187] Typically, it is difficult to reproducibly target each, phase-pure micelle morphology. Therefore, phase diagrams were constructed for a given degree of polymerization (DP_n) of the "A" block by increasing the length of the "B" block and varying the copolymer concentration. This perspective aims to provide an overview of selected recent advances using PISA. For a more detailed overview the reader is referred to the relevant references.[19, 20, 184, 188]

5.2 PISA formulations that use different controlled radical polymerization techniques.

Important examples of controlled radical polymerization methods include NMP, ATRP, and RAFT polymerization.[25-27] PISA involving nitroxide-mediated aqueous emulsion polymerization was used to prepare amphiphilic diBCPs based on methacrylic acid and

methyl methacrylate, which can self-assemble into spheres, worm-like micelles or vesicles, mainly depending on the length (volume fraction) of the hydrophobic PMMA block.[189, 190] PISA formulations can be also based on ATRP. During the polymerization of PEO-*b*-(4VP-*co*-MBA) (4VP = 4-vinylpyridine, MBA = *N,N'*-methylenebisacrylamide) diBCPs in an ethanol/water mixture, the BCPs self-assembled in situ to form spherical micelles consisting of a P4VP-*co*-MBA core and a PEO corona.[191] PISA of BCPs has been, however, most intensively applied using RAFT polymerization, both in organic and aqueous media and often yielding very high monomer conversions. This approach will be highlighted in the rest of the section below.

Two different types of RAFT polymerization exist that are applicable to PISA: aqueous emulsion polymerization and aqueous dispersion polymerization. The RAFT aqueous emulsion process is initiated from a water-soluble macromolecule, using water-immiscible monomers, e.g. *n*-butyl acrylate, methyl methacrylate, and styrene.[192, 193] The RAFT-mediated emulsion polymerization of *n*-butyl acrylate as well as the copolymerization of *n*-butyl acrylate and methyl methacrylate from PEO macroinitiators yielded stable, submicrometer-sized diBCP nanoparticles.[192] By selecting an appropriate PEO-based macroinitiator, the polymerization control of PEO-*b*-PS as well as the nanoparticle size distribution were improved.[193]

Compared to RAFT aqueous emulsion polymerizations, water-miscible vinyl monomers are used for RAFT aqueous dispersion polymerizations to synthesize the core-forming blocks.[20] Functional vinyl monomers include N-isopropylacrylamide (NIPAM),[194, 195] N,N'-diethylacrylamide (DEAA),[196-198] 2-methoxyethyl acrylate (MEA),[199, 200] 2-hydroxypropyl methacrylate (HPMA),[201, 202] and di(ethylene glycol) methyl ether methacrylate (DEGMA)[203] (see Figure 13a). The growing, second block drives the in situ self-assembly of the micelles,

which are sterically stabilized by the water-soluble macroinitiator. Except for the case of HPMA, all core-forming monomers mentioned above led to spherical micelles.[194, 196-199] In addition, both high monomer conversions of >99% and high blocking efficiencies (i.e. high fractions of BCPs compared to the fraction of homopolymer impurities) of ≥90% make HPMA an interesting core-forming monomer. RAFT aqueous dispersion polymerizations of HPMA are initiated from PGMA, PMPC, or PEO macroinitiators.[1, 202] During the polymerization, the hydrophobic poly(2-hydroxypropyl methacrylate) (PHPMA) block length increases gradually, leading to a progressive change of the nanoparticle morphology from spheres-to-worms-to-vesicles. In order to target pure micelle morphologies, phase diagrams for PGMA-*b*-PHPMA diBCP were constructed, keeping the PGMA block lengths constant and increasing the PHMPA block lengths, as well as varying the copolymer concentration between 10% and 25% w/w (see Figure 13b and c).[1, 48, 201] TriBCP vesicles have been synthesized via RAFT aqueous dispersion polymerization by adding, for example, benzyl methacrylate (BzMA) to a solution of PGMA-*b*-PHPMA copolymer vesicles, which no longer contained significant amounts of HPMA monomer. This reaction resulted in the formation of well-defined, framboidal vesicles due to the enthalpic incompatibility of both core-forming blocks and subsequent microphase separation (see Figure 13d).[204]

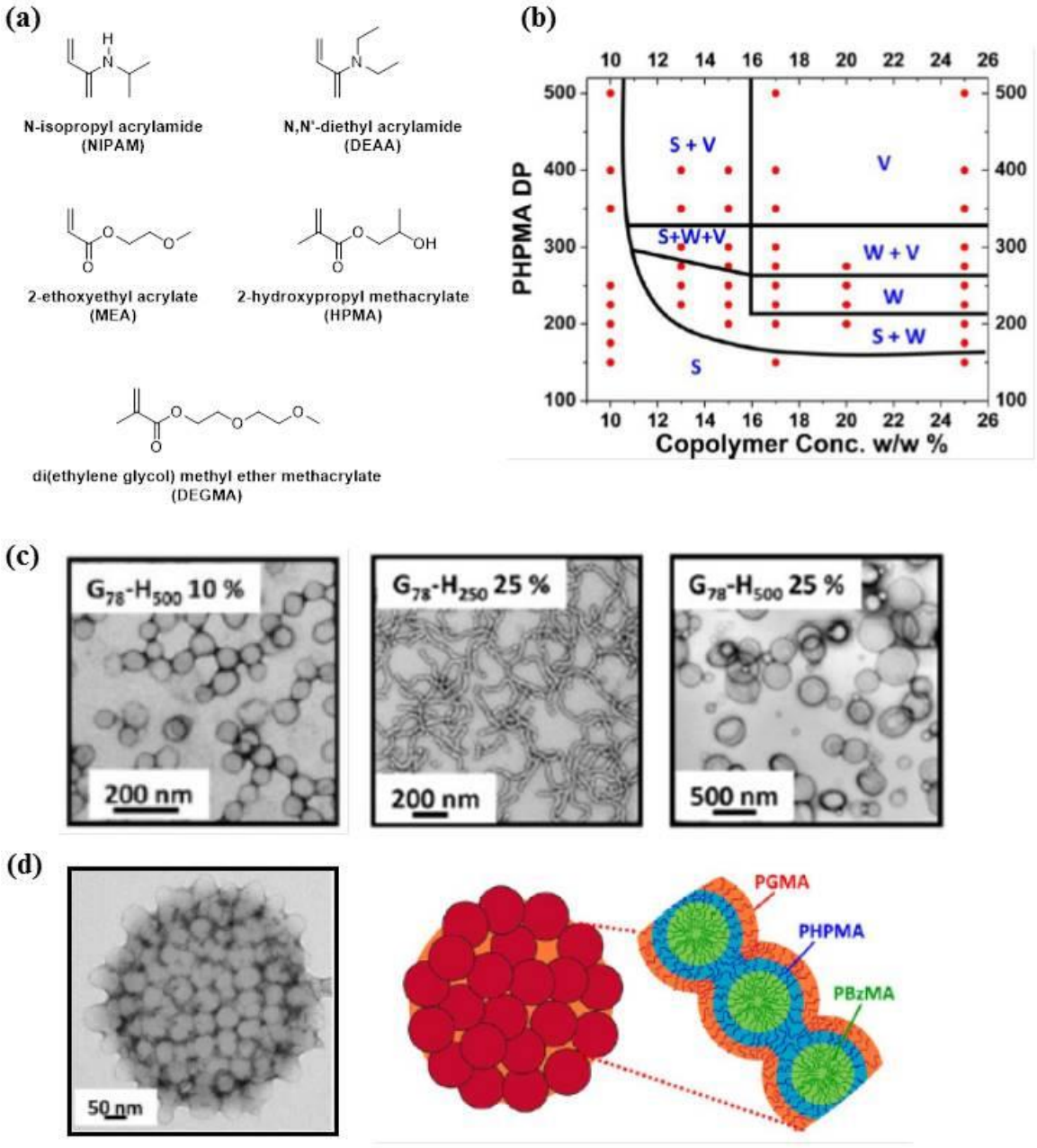

Figure 13. (a) Vinyl monomers which are suitable for PISA by RAFT aqueous dispersion polymerization. (b) Phase diagram and (c) example TEM images for a series of $PGMA_{78}$-*b*-$PHPMA_x$ diBCPs obtained by RAFT aqueous dispersion polymerization (copolymer concentration varied between 10 and 25% w/w; S = spheres, W = worm-like micelles, V = vesicles). (d) TEM micrograph of a $PGMA_{58}$-*b*-$PHPMA_{350}$-*b*-$PBzMA_{200}$ triBCP framboidal vesicle and schematic illustration of the likely spatial locations of the three polymer blocks after microphase-separation. Reproduced with permission from ref. [20] (copyright 2014 American Chemical Society), ref. [201] (copyright 2012 American Chemical Society), and ref. [204] (copyright 2012 American Chemical Society).

The growth of spherical micelles during the RAFT alcoholic dispersion polymerization of BzMA, initiated with poly(2-(dimethylamino)ethylmethacrylate) (PDMA), has been studied by a variety of techniques.[205] This revealed that growth of these spherical micelles results

from the combination of an increase in DP_n of BzMA, an exchange of BCP chains between micelles and fusion of micelles.

The evolution of the particle morphology during the RAFT aqueous dispersion polymerization of PGMA-*b*-PHPMA diBCPs was studied by DLS and TEM.[202] The increase in PHMPA block length and the in situ self-assembly of the diBCPs led to spheres, worm-like micelles and vesicles within a reaction time of 2 h (>99% monomer conversion, high mass percentage of solids in pure water). The sphere-to-worm and worm-to-vesicle transitions were accompanied by different intermediate structures, e.g. "octopi" and "jellyfish" which were observed during the worm-to-vesicle transition (see Figure 14). To be more precise, the morphological worm-to-vesicle transition during the synthesis and self-assembly of $PGMA_{47}$-*b*-$PHPMA_{200}$ was observed to occur via a five-step mechanism. The initial 1D linear worm-like micelles (68% monomer conversion, $PGMA_{47}$-*b*-$PHPMA_{131}$) formed branched worm-like micelles, developing in a subsequent step to highly branched worm-like structures accompanied by a swelling of the junction points. These so-called "octopi" structures can partially coalesce and can form nascent bilayers with "tentacles". Subsequently, the bilayers can wrap up to form jellyfish "tentacle"-like structures which then undergo fusion to form pure vesicles when high monomer conversions are achieved (>99%, $PGMA_{47}$-*b*-$PHPMA_{200}$).[202] The "jellyfish" intermediate structure was also observed during the RAFT dispersion polymerization of BzMA in ethanol initiated from PHPMA, as well as during post-polymerization reactions of BCPs.[20, 206] This suggests that the "jellyfish" intermediate morphology is a generic structure for the self-assembly of BCPs. The morphological transitions from spheres-to-worms-to-vesicles can be predicted by the packing parameter[38,48] However, for quantitative predictions of diBCP micelle morphologies, further parameters, such as the degree of solvation of the core-forming block by water molecules and non-

converted monomers have to be taken into account, the latter one in particular for RAFT polymerizations with incomplete monomer conversions.[19]

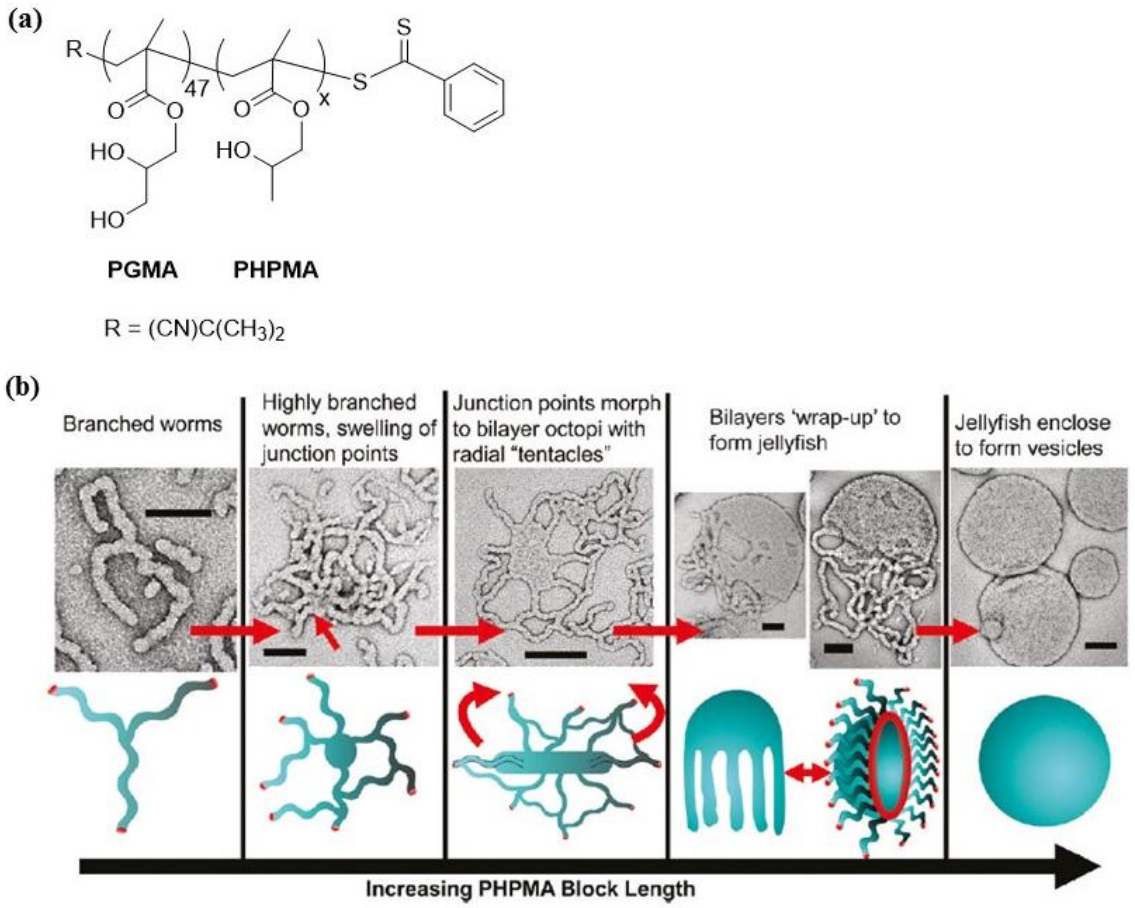

Figure 14. (a) Chemical structure of poly[(glycerol monomethacrylate)-*b*-(2-hydroxypropyl methacrylate)] ($PGMA_{47}$-*b*-$PHPMA_x$). (b) Suggested mechanism for the morphological worm-to-vesicle transition during the RAFT aqueous dispersion polymerization of $PGMA_{47}$-*b*-$PHPMA_{200}$. Reproduced with permission from ref. [202] (copyright 2011 American Chemical Society).

5.3 PISA with crystallisable core-forming blocks: Combining PISA with living CDSA.

PISA syntheses have been dominated to date by the use of amorphous core-forming blocks. The use of a crystallizable core-forming block offers more convenient access to non-spherical morphologies such as cylinders/fibers and platelets, which possess potential advantages for many applications. PISA syntheses of BCP micelles with a variety of crystallizable cores have also been reported. For example, highly concentrated dispersions of cylinders from BCP containing liquid crystalline cholesteryl moieties[207] and semicrystalline poly(stearyl

methacrylate) cores[208] have been described. In addition, elongated micelles with crystalline polythiophene[131, 209] and polyacetylene[130] core-forming blocks have also been described.

In a further breakthrough, a rapid and convenient preparation of cylindrical and platelet BCP micelles at concentrations up to 25% w/w solids has been achieved by the coupling of established PISA and CDSA protocols, in a process termed "PI-CDSA" for PFDMS BCPs as an illustrative case.[210] Moreover, the living CDSA approach can be applied, allowing access to monodisperse cylindrical micelles of controlled length. The latter involved a one-pot process in which living PI was added to a ferrocenophane monomer in the presence of small seed micelles to lead to synchronous polymerization, crystallization, and self-assembly. Uniform cylinders with lengths up to ca. 3 microns were prepared. This proof of concept work focussed on the use of anionic polymerisation and BCPs based on PFDMS. Clearly, PI-CDSA should be extendable to other BCPs with crystalline core-forming blocks that can be prepared by this well-developed polymerisation protocol. The success of the PI-CDSA approach even under the stringent conditions required for living anionic polymerisations suggests a potentially general applicability of this method to other crystallisable BCPs that can be prepared by other living/controlled polymerisation processes.[210]

6. Properties and Applications of BCP micelles

6.1 Stability considerations

In the previous sections the preparation of BCP micelles and the factors that control their morphology and dimensions were discussed. This section focuses on the properties and applications of BCP micelles prepared via solution self-assembly of BCPs, and again our approach is to illustrate selected, but representative examples.

An important feature of BCP micelles is their relative stability compared to those formed by low molar mass analogues such as molecular surfactants and lipids. For example, the robustness of BCP vesicles compared to lipid-based examples has been demonstrated by their enhanced toughness and increased areal strain before rupture.[211] Such membrane stability is, for example, essential for avoiding uncontrolled release of drugs due to formation of cracks in an early stage of treatment.[212] As a result of their stability, BCP micelles are promising for a broad range of different applications,[1, 6, 17, 62, 213] especially when compositional chemistries and functionality are used to promote useful characteristics such as biocompatibility or stimuli-responsiveness towards external triggers. Furthermore, where needed, micelle structural integrity can be enhanced further by core- or corona crosslinking, which makes the structures permanent and allows their dispersion in a wide variety of media (see section 2).

6.2 Biomedical applications

(i) Drug delivery and release.

BCP micelles are highly promising as delivery vehicles for biomedical applications and many detailed reviews exist.[1, 6, 7, 11, 12, 16, 17, 62, 213, 214] The hydrophobic micelle core can solubilize and absorb hydrophobic active components, and both the hydrophobic core and the hydrophilic corona can be composed of biocompatible polymers. Multicompartment micelles offer the possibility of segregated storage and the release of different actives at the same time or sequentially.[13] Pluronics (also known as poloxamers) are hydrophilic, non-ionic triblock copolymers consisting of a central hydrophobic block of polypropylene oxide flanked by two hydrophilic blocks of PEO. These have a broad variety of commercial applications as surfactants and as solubilizers for hydrophobic species in aqueous media such as drugs and cosmetics.[215, 216]

PEO is of high interest as a corona-forming polymer with biodegradable PLA or PCL as core-forming materials. For example, the use of PEO-*b*-PLA vesicles that were loaded with two different anti-cancer drugs has led to improved drug efficacy and tumor cytotoxicity. The hydrophilic and hydrophobic components were both encapsulated into the vesicles, which released the drugs within one day and increased the cell death in tumors by a factor of two compared to an exposure with the free drugs.[217, 218] In addition, 1D and 2D micelles with a crystalline PLA or PCL core have shown potential in biomedical applications.[110, 111, 148, 166, 167, 219-223]

Chemical functionalization of the micelle core and corona affects the interaction between the micelle and the cell surface, as well as the efficiency of drug uptake and release. For example, PEO-*b*-PLA micelles have been functionalized with ligands which can bind to $\alpha_v\beta_3$ integrins and consequently used to target the drug delivery.[224] An anticancer drug (doxorubicin) and superparamagnetic iron oxide nanoparticles, both initially encapsulated into the micelle core, were successfully delivered to $\alpha_v\beta_3$-expressing tumor cells. In addition to chemical functionalization, micelle morphology and dimensions, i.e. shape and size, can influence the blood circulation time,[225] the rate of cell internalization and exit,[226, 227] and the efficacy for drug delivery.[228-230] 1D and 2D micelles exhibiting precisely controlled dimensions can be obtained by living CDSA (see section 4) and this suggests promising possibilities to tailor anisotropic micelles for drug delivery.

For maximum efficiency, controlled release of the active components is required once the targeted location has been reached. It has been successfully demonstrated that BCP micelles are able to control the release of the gaseous therapeutic carbon monoxide (CO) or nitric oxide (NO) under physiological conditions.[231, 232] For example, spherical, CO-releasing micelles formed from triBCPs consisting of a hydrophobic poly(*n*-butylacrylamide) block, a hydrophilic PEO block, and a poly(ornithine acrylamide) block, which carried the

hydrophilic, CO releasing $Ru(CO)_3Cl$(ornithinate) moiety, have been prepared in aqueous solution. CO release was triggered by thiol-containing species, such as cysteine. However, this was only observed when exposing the micelles to an appropriately high concentration of cysteine, which exists, for example, in the endosome/lysosome compartment of mammalian cell lines;[233, 234] in contrast, the cysteine concentration is significantly lower in the blood plasma. These CO-releasing micelles are therefore of interest for therapeutic applications, especially as the stealth behaviour of PEO led to a drastic decrease in toxicity for the $Ru(CO)_3Cl$(ornithinate) moiety.[232]

(ii) Antibacterial Activity

Antimicrobial activity is a further highly desirable property of intense current interest. This has been achieved for PAA-*b*-PS micelles containing silver ions and/or N-heterocyclic carbene-silver complexes.[235] These micelles were found to function as antimicrobial agents against *Escherichia coli* and *Pseudomonas aeruginosa* bacteria. The antimicrobial activity of a cationic worm-gel (a gel of cylindrical micelles) has also been investigated towards *Staphylococcus aureus* bacteria.[236] The cationic diBCP worm-like micelles were prepared via PISA by RAFT aqueous dispersion polymerization of HPMA, initiated with a mixture of cationic PQDMA (poly(2-(methacryloyloxy)ethyl)trimethylammonium chloride) and non-ionic PGMA macroinitiators (molar ratio of 1:9). Compared to the non-ionic $PGMA_{62}$-*b*-$PHPMA_{200}$ worm-gel, the cationic ($0.95PGMA_{62}$ + $0.05PQDMA_{95}$)-*b*-$PHPMA_{200}$ worm-gel was found to be bacteriostatic and exhibited a mildly bactericidal behavior.

6.2 Stimuli-responsive materials.

BCP micelles can be designed to be able to respond to various environmental triggers, e.g. to changes in temperature or pH, to irradiation with light of a specific wavelength, or to additives, such as oxidants and reductants. Considering their enhanced robustness compared

to lipid-based micelles, stimuli-responsive, non-toxic BCP micelles are considered promising systems for delivery applications and, in particular, as multi-responsive materials where a range of actions can be controlled by different external triggers.[237]

Thermo-responsive polymers change their solubility upon a change in temperature. On heating a solution above a critical temperature (lower critical solution temperature, LCST) or cooling a solution below a critical temperature (upper critical solution temperature, UCST), a variety of polymers are able to change their solution behavior, for example, by switching from hydrophilic to hydrophobic. PEO, PVA, PHEMA and PNIPAAM and poly(alkyloxazolines) exhibit LCST behavior and poly(*N*-acryloylasparaginamide) is a polymer with UCST behavior.[238] Thermoreversible gelation was observed for diBCP micelles prepared via PISA by RAFT dispersion polymerization in polar[239] and non-polar[240] organic solvents as well as in water.[241] $PDMA_{20}$-*b*-$PPPMA_{47}$ (PPPMA = poly(3-phenylpropyl methacrylate)) worm-like micelles were prepared by PISA in ethanol and a free-standing gel was obtained at room temperature and 21% w/w solids.[239] On heating the dispersion to 70 °C, degelation took place and a fluid was obtained. This was caused by a reversible worm-to-sphere transition as worm-like micelles are able to interact with each other more efficiently than spherical micelles. A thermo-responsive worm-gel was also obtained for a 20% w/w $PLMA_{16}$-*b*-$PBzMA_{37}$ micelle dispersion in dodecane (Figure 15a and b).[240] Upon heating this dispersion to 90 °C, degelation occurred again due to a worm-to-sphere transition. The transition occurs, however, via sequential budding rather than random worm cleavage (Figure 15c) and is reversible in concentrated solution of 20 % w/w, but irreversible in diluted solutions of 0.1 % w/w. It was not necessary to convert all BCP worm-like micelles into spherical micelles in order to induce degelation. At an increased temperature, the core-forming PBzMA block is partially solvated and surface plasticization takes place, leading to an increase in the volume fraction of the corona-forming PLMA block, a reduction of the packing parameter and, consequently, a change of the micelle morpholgy.[240] Combination of a worm-like micelle forming BCP which

undergoes the gel-to-fluid transition together with an ice-inhibiting polymer, poly(vinyl alcohol), to prevent ice crystal formation during thawing has led to a promising matrix for the solvent-free cryopreservation of red blood cells. Potential applications in storage and transport exist and also for tissue engineering, where in situ gelation is desirable.[242]

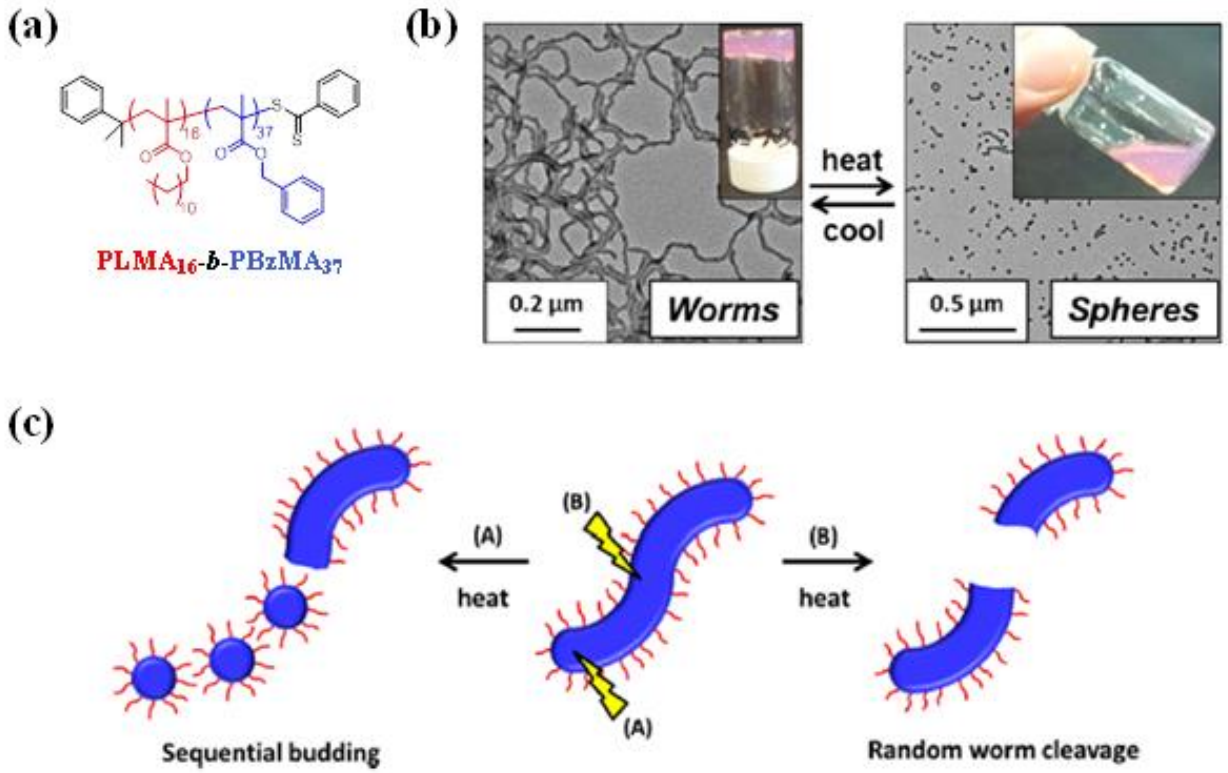

Figure 15. (a) Chemical structure of $PLMA_{16}$-*b*-$PBzMA_{37}$. (b) Thermoresponsive solution behavior of $PLMA_{16}$-*b*-$PBzMA_{37}$ micelles in dodecane at 20 % w/w solids. (c) Scheme of possible mechanisms (sequential budding (i) vs. random worm cleavage (ii)) for the degelation via a worm-to-sphere transition when heating $PLMA_{16}$-*b*-$PBzMA_{37}$ worm-like micelles dispersed in dodecane. Reproduced with permission from ref. [240] (copyright 2014 American Chemical Society).

The thermoreversible gelation of a PBLG-containing diBCP conjugate (PBLG = poly(γ-benzyl-L-glutamate), namely PFDMS-*b*-PBLG, has also been observed in dilute solution.[243] By cooling a PFDMS-*b*-PBLG solution in toluene to ambient temperature, an optically transparent gel formed. The authors proposed a new mechanism for gelation for these BCPs. Thus, polymers form nanoribbons which self-assemble in a monolayer fashion involving strong dipolar π-π interactions induced by the phenyl groups between the PBLG helices.

Light-responsive micelles were prepared from PAzoMA-*b*-PAA diBCPs (PAzoMA = azobenzene-containing polymethacrylate). Reversible disassembly and re-assembly of the BCP micelles in a water/dioxane solution was induced by alternating the illumination with UV and visible light. This phenomenon results from the reversible *trans*-*cis* photoisomerization of the azobenzene moieties located in the PAzoMA micelle core.[244]

Redox-active organometallic vesicles composed of a hydrophilic, electroactive PFDMS polyelectrolyte corona-forming block and a hydrophobic PDMS block have been prepared in aqueous medium.[245] These micelles have potential applications in terms of redox-tunable encapsulations. Reversible, redox-controlled micellization was observed for a series of PFDMS-*b*-PS diBCPs, where PFDMS can be poly(ferrocenylphenylmethylsilane), poly(ferrocenylethylmethylsilane) or PFDMS..[246] The redox properties of cylindrical PFDMS-*b*-PI micelles with a crystalline PFDMS micelle core and a solvent-swollen PI corona have also been studied.[247] After corona cross-linking and pre-oxidation of the PFDMS core segment, silver ions were then reduced by reaction with the remaining Fe(II) centers, leading to the formation of nanowires with silver nanoparticles within the micelle core.[247] Responsive anisotropic particles such as ellipsoids and nanosheets based on PFS-b-P2VP have also been studied and these exhibit substantial morphology changes on exposure to oxidants.[248]

6.3 Solution templating and the creation of hybrid materials.

PFDMS-*b*-P2VP micelles with a crystalline PFDMS core prepared by living CDSA have been used as templates for the synthesis of continuous or segmented nanowire structures.[179] These element oxide/conducting polymer-based nanowires were obtained via a sol-gel process upon depositing the element alkoxide precursors within the micelle corona in an isopropanol/water mixture. PFDMS-*b*-P2VP triblock comicelles exhibiting a spatially defined charge on the

P2VP corona resulted in the formation of a segmented element oxide coating of the cylindrical micelles due to electrostatic interactions between the hydrolyzed metal anions and the cationic P2VP blocks. In addition, inorganic nanowire replicas were achieved by calcination.[179]

Bio-inspired organic-inorganic hybrid structures have been synthesized by using anionic PMAA-*b*-PBzMA micelles. These micelles act as "pseudo-proteins" and were incorporated into single crystals of calcite, resulting in hybrid materials with enhanced mechanical properties compared to pure calcite crystals.[249] The occlusion mechanism was investigated in detail, including the specific binding of polymer micelle on calcite, compression of the micelle during the occlusion, and the formation of a cavity.[250] In addition, BCP micelles with an optimum rather than a maximum surface density of the anionic stabilizer chains were found to bind to calcite efficiently and their extent of incorporation into the crystals was significantly higher.[251]

6.4 Etch resists in nanolithography and functional nanostructures for devices

Thin BCP films exhibiting a periodic patterning on the length scale ≤ 50 nm are of interest for applications in ultrahigh resolution lithography.[252-254] In this context, continuous ceramic nanolines with length of a few micrometers and widths down to 8-30 nm were created by depositing a solution of cylindrical PFDMS-*b*-PDMS or PFDMS-*b*-PI micelles with crystalline cores onto a semiconducting substrate, followed by reactive ion etching.[255] Another example is the use of monodisperse cylindrical PFDMS-b-P2VP micelles with crystalline cores in the template-directed synthesis of colloidally stable, electrically conductive polyaniline nanofibers.[180] In this approach the cylindrical BCP micelles were stabilized by forming an oligomeric aniline coating. By addition of a polymeric acid dopant, doped polyaniline nanofibers formed exhibiting the shape of the initial micellar templates. These nano-objects may be of interest for nanoscale electronic devices. In the context of

enhanced carrier mobility and high-performance electro-optical devices, hybrid nanowires with well-defined donor/acceptor interfaces are of major interest. N-type quantum dots or fullerenes and p-type P3HT-containing BCPs have been used to form hybrid nanowires by solution processing routes.[256-258]

6.5 Applications of BCP micelles for lubrication and composite reinforcement, and as stabilizers.

PISA of PLMA-*b*-PBzMA has been studied in industrially-sourced mineral oil as well as in poly(α-olefin) oil which is an industrially-relevant solvent.[259] PISA in industrially-sourced mineral oil led to the formation of spheres, worm-like micelles, and vesicles (provided that the DP_n of PLMA was kept sufficiently low) and the phase diagram, for which the DP_n of PBzMA and the polymer concentration were varied, was similar to the one constructed for the same BCP in dodecane.[240] When using poly(α-olefin) oil as a solvent for PISA of PLMA-*b*-PBzMA, the boundaries of the phase diagram differed from the ones in mineral oil and dodecane, however, pure sphere, worm-like, and vesicle morphologies were accessible. For a PISA formulation of $PLMA_{50}$-*b*-$PBzMA_{100}$ that yields spherical micelles, a "one-pot" synthetic approach was developed. This involved the synthesis of the PLMA macroinitiator by RAFT solution polymerization in mineral oil, followed by RAFT dispersion polymerization of BzMA in the same reaction medium. In both steps, high monomer conversion of >95% and high blocking efficiencies were achieved. Spherical micelles prepared from methacrylic-containing BCPs may function as lubricity modifiers for base automotive engine oils.[260] In this context, RAFT polymerization techniques might play a leading role in the future.[261, 262]

Micelles formed from amphiphilic BCPs are able to lead to an enhanced fracture resistance of epoxy resins when incorporated into the epoxy matrix.[263, 264] For example, low molecular

weight PHO-*b*-PEO (PHO = poly(hexylene oxide)) micelles were used as an additive for the toughening of epoxy resins. Depending on the composition of the diBCP, spheres, worm-like micelles and vesicles formed in the epoxy matrix, leading to binary epoxy/polymer blends which contain 5 wt% of BCP. PHO was proposed to induce segregation between both blocks as well as segregation with epoxy.[264]

BCP micelles can be used as hydrophobic Pickering emulsifiers, stabilizing water-in-oil emulsions. Hydrophobic $PLMA_{16}$-*b*-$BzMA_{37}$ worm-like micelles act more efficiently as emulsifiers than hydrophobic spheres composed of the same BCP, as worm-like morphologies led to the formation of smaller, more stable droplets in water-in-*n*-dodecane emulsions.[265] By using a combination of hydrophilic and hydrophobic worm-like micelles, highly stable Pickering double emulsions with water or oil as the continuous phase were prepared, which were confirmed by fluorescence spectroscopy.[266] This BCP also allowed for preparing non-aqueous Pickering emulsions, replacing water by ethylene glycol. Near-isorefractive emulsions with a transmittance of 81% across the visible spectral range were obtained by emulsifying ethylene glycol with *n*-tetradecane by using a dispersion of $PLMA_{16}$-*b*-$BzMA_{37}$ worm-like micelles in tetradecane.[267]

7. Summary

The discovery of living anionic polymerization in the 1950s and, controlled radical polymerization methods in the 1990s represent crucial developments for the preparation of well-defined BCPs and subsequent studies of their solution self-assembly behavior. Work on "crew-cut" micelles in the mid 1990s established predictable morphological diversity for BCPs in selective solvents and many of the key factors that influence morphological transitions.

More recent work has focused on multicompartmental micelles and hierarchical structures of increasingly remarkable complexity. As revealed in this Perspective, a myriad of approaches

involving thermodynamic and kinetic control have been used with diBCP and also triBCPs with various geometris to create a wonderland of new morphologies. The use of structurally different BCP building blocks is also of continuing interest. For example, an exciting emerging area involves the self-assembly of branched-linear BCPs in which the packing parameter exceeds unity as the resulting flat bilayer is anticipated to develop negative curvature. This can result in the formation of cubosomes, nanoporous colloidal nanoparticles consisting of inverse bicontinuous cubic phases of BCP bilayers. These assemblies have potential applications in separation and release.[268-271]

The preparation of non-spherical 1D and 2D morphologies with controlled dimensions by the use of crystalline core-forming blocks offers promise in several areas, especially if the living CDSA approach can be extended to a broad range of functional BCP materials. From a more applied perspective, large scale preparations using the PISA approach where polymerization and self-assembly are carried out without isolation of the intermediate BCP offers feasible applications across a diverse range of fields from composites to the life sciences. These considerations all strongly suggest that the future of the field of BCP solution self-assembly is very bright from both a fundamental and an applied scientific perspective.

References

1. Blanazs, A.; Armes, S. P.; Ryan, A. J. *Macromolecular Rapid Communications* **2009,** 30, (4-5), 267-277.
2. Hamley, I., *Block Copolymers in Solution: Fundamentals and Applications*. Wiley: Chichester, 2005.
3. Gohy, J.-F. *Advances in Polymer Science* **2005,** 190, 65-136.
4. Hamley, I. W. *Angewandte Chemie International Edition* **2003,** 42, (15), 1692-1712.
5. Hadjichristidis, N.; Pispas, S.; Floudas, G., *Block Copolymers: Synthetic Strategies, Physical Properties, and Applications*. Wiley: Hoboken, 2002.
6. Schacher, F. H.; Rupar, P. A.; Manners, I. *Angewandte Chemie International Edition* **2012,** 51, (32), 7898-7921.
7. Mitragotri, S.; Anderson, D. G.; Chen, X.; Chow, E. K.; Ho, D.; Kabanov, A. V.; Karp, J. M.; Kataoka, K.; Mirkin, C. A.; Petrosko, S. H.; Shi, J.; Stevens, M. M.; Sun, S.; Teoh, S.; Venkatraman, S. S.; Xia, Y.; Wang, S.; Gu, Z.; Xu, C. *ACS Nano* **2015,** 9, (7), 6644-6654.
8. Bates, F. S.; Hillmyer, M. A.; Lodge, T. P.; Bates, C. M.; Delaney, K. T.; Fredrickson, G. H. *Science* **2012,** 336, (6080), 434-440.
9. Lodge, T. P.; Ueki, T. *Accounts of Chemical Research* **2016,** 49, (10), 2107-2114.
10. Elsabahy, M.; Wooley, K. L. *Accounts of Chemical Research* **2015,** 48, (6), 1620-1630.
11. Elsabahy, M.; Heo, G. S.; Lim, S.-M.; Sun, G.; Wooley, K. L. *Chemical Reviews* **2015,** 115, (19), 10967-11011.
12. Sakai-Kato, K.; Nishiyama, N.; Kozaki, M.; Nakanishi, T.; Matsuda, Y.; Hirano, M.; Hanada, H.; Hisada, S.; Onodera, H.; Harashima, H.; Matsumura, Y.; Kataoka, K.; Goda, Y.; Okuda, H.; Kawanishi, T. *Journal of Controlled Release* **2015,** 210, 76-83.
13. Moughton, A. O.; Hillmyer, M. A.; Lodge, T. P. *Macromolecules* **2012,** 45, (1), 2-19.
14. Truong, N. P.; Quinn, J. F.; Whittaker, M. R.; Davis, T. P. *Polymer Chemistry* **2016,** 7, (26), 4295-4312.
15. Lodge, T. P. *Macromolecular Chemistry and Physics* **2003,** 204, (2), 265-273.
16. Ge, Z.; Liu, S. *Chemical Society Reviews* **2013,** 42, (17), 7289-7325.
17. Rodríguez-Hernández, J.; Chécot, F.; Gnanou, Y.; Lecommandoux, S. *Progress in Polymer Science* **2005,** 30, (7), 691-724.
18. Mai, Y.; Eisenberg, A. *Chemical Society Reviews* **2012,** 41, (18), 5969-5985.
19. Derry, M. J.; Fielding, L. A.; Armes, S. P. *Progress in Polymer Science* **2016,** 52, 1-18.
20. Warren, N. J.; Armes, S. P. *Journal of the American Chemical Society* **2014,** 136, (29), 10174-10185.
21. Szwarc, M.; Levy, M.; Milkovich, R. *Journal of the American Chemical Society* **1956,** 78, (11), 2656-2657.
22. Szwarc, M. *Nature* **1956,** 178, (4543), 1168-1169.
23. Newman, S. *Journal of Applied Polymer Science* **1962,** 6, (21), S15-S16.
24. Krause, S. *The Journal of Physical Chemistry* **1964,** 68, (7), 1948-1955.
25. Matyjaszewski, K.; Xia, J. *Chemical Reviews* **2001,** 101, (9), 2921-2990.
26. Hawker, C. J.; Bosman, A. W.; Harth, E. *Chemical Reviews* **2001,** 101, (12), 3661-3688.
27. Moad, G.; Rizzardo, E.; Thang, S. H. *Australian Journal of Chemistry* **2006,** 59, (10), 669-692.
28. Braunecker, W. A.; Matyjaszewski, K. *Progress in Polymer Science* **2007,** 32, (1), 93-146.
29. Patten, T. E.; Matyjaszewski, K. *Advanced Materials* **1998,** 10, (12), 901-915.
30. Moad, G.; Rizzardo, E.; Thang, S. H. *Australian Journal of Chemistry* **2005,** 58, (6), 379-410.
31. Tantakitti, F.; Boekhoven, J.; Wang, X.; Kazantsev, R. V.; Yu, T.; Li, J.; Zhuang, E.; Zandi, R.; Ortony, J. H.; Newcomb, C. J.; Palmer, L. C.; Shekhawat, G. S.; de la Cruz, M. O.; Schatz, G. C.; Stupp, S. I. *Nat Mater* **2016,** 15, (4), 469-476.
32. Hoogenboom, R.; Schlaad, H. *Polymer Chemistry, accepted* **2016**.
33. Freeman, R.; Boekhoven, J.; Dickerson, M. B.; Naik, R. R.; Stupp, S. I. *MRS Bulletin* **2015,** 40, (12), 1089-1101.

34. Aida, T.; Meijer, E. W.; Stupp, S. I. *Science* **2012,** 335, (6070), 813-817.
35. Hamley, I. W.; Castelletto, V. *Bioconjugate Chemistry, accepted* **2016**.
36. Hamley, I. W. *Angewandte Chemie International Edition* **2014,** 53, (27), 6866-6881.
37. Biedermann, F.; Nau, W. M.; Schneider, H.-J. *Angewandte Chemie International Edition* **2014,** 53, (42), 11158-11171.
38. Israelachvili, J. N.; Mitchell, D. J.; Ninham, B. W. *Journal of the Chemical Society, Faraday Transactions 2: Molecular and Chemical Physics* **1976,** 72, (0), 1525-1568.
39. Karayianni, M.; Pispas, S., Self-Assembly of Amphiphilic Block Copolymers in Selective Solvents. In *Fluorescence Studies of Polymer Containing Systems*, Procházka, K., Ed. Springer International Publishing: Cham, 2016; pp 27-63.
40. Hayward, R. C.; Pochan, D. J. *Macromolecules* **2010,** 43, (8), 3577-3584.
41. Cameron, N. S.; Corbierre, M. K.; Eisenberg, A. *Canadian Journal of Chemistry* **1999,** 77, (8), 1311-1326.
42. Cui, H.; Chen, Z.; Wooley, K. L.; Pochan, D. J. *Soft Matter* **2009,** 5, (6), 1269-1278.
43. Riess, G. *Progress in Polymer Science* **2003,** 28, (7), 1107-1170.
44. Jain, S.; Bates, F. S. *Science* **2003,** 300, (5618), 460-464.
45. Discher, D. E.; Eisenberg, A. *Science* **2002,** 297, (5583), 967-973.
46. Won, Y.-Y.; Davis, H. T.; Bates, F. S. *Science* **1999,** 283, (5404), 960-963.
47. Jain, S.; Bates, F. S. *Macromolecules* **2004,** 37, (4), 1511-1523.
48. Antonietti, M.; Förster, S. *Advanced Materials* **2003,** 15, (16), 1323-1333.
49. Guo, A.; Liu, G.; Tao, J. *Macromolecules* **1996,** 29, (7), 2487-2493.
50. Thurmond, K. B.; Kowalewski, T.; Wooley, K. L. *Journal of the American Chemical Society* **1996,** 118, (30), 7239-7240.
51. Thurmond, K. B.; Kowalewski, T.; Wooley, K. L. *Journal of the American Chemical Society* **1997,** 119, (28), 6656-6665.
52. Wooley, K. L. *Chemistry – A European Journal* **1997,** 3, (9), 1397-1399.
53. Ding, J.; Liu, G. *Macromolecules* **1998,** 31, (19), 6554-6558.
54. Wang, X.; Liu, K.; Arsenault, A. C.; Rider, D. A.; Ozin, G. A.; Winnik, M. A.; Manners, I. *Journal of the American Chemical Society* **2007,** 129, (17), 5630-5639.
55. O'Reilly, R. K.; Hawker, C. J.; Wooley, K. L. *Chemical Society Reviews* **2006,** 35, (11), 1068-1083.
56. Selb, J.; Gallot, Y. *Die Makromolekulare Chemie* **1980,** 181, (12), 2605-2624.
57. Canham, P. A.; Lally, T. P.; Price, C.; Stubbersfield, R. B. *Journal of the Chemical Society, Faraday Transactions 1: Physical Chemistry in Condensed Phases* **1980,** 76, (0), 1857-1867.
58. Hilfiker, R.; Wu, D. Q.; Chu, B. *Journal of Colloid and Interface Science* **1990,** 135, (2), 573-579.
59. Zhang, L.; Eisenberg, A. *Science* **1995,** 268, (5218), 1728-1731.
60. Zhang, L.; Yu, K.; Eisenberg, A. *Science* **1996,** 272, (5269), 1777-1779.
61. Zhang, L.; Eisenberg, A. *Journal of the American Chemical Society* **1996,** 118, (13), 3168-3181.
62. Groschel, A. H.; Muller, A. H. E. *Nanoscale* **2015,** 7, (28), 11841-11876.
63. Lunn, D. J.; Finnegan, J. R.; Manners, I. *Chemical Science* **2015,** 6, (7), 3663-3673.
64. Wang, L.; Lin, J.; Zhang, X. *Polymer* **2013,** 54, (14), 3427-3442.
65. Skrabania, K.; Berlepsch, H. v.; Böttcher, C.; Laschewsky, A. *Macromolecules* **2010,** 43, (1), 271-281.
66. Laschewsky, A. *Current Opinion in Colloid & Interface Science* **2003,** 8, (3), 274-281.
67. Li, Z.; Kesselman, E.; Talmon, Y.; Hillmyer, M. A.; Lodge, T. P. *Science* **2004,** 306, (5693), 98-101.
68. Li, Z.; Hillmyer, M. A.; Lodge, T. P. *Langmuir* **2006,** 22, (22), 9409-9417.
69. Jang, S. G.; Audus, D. J.; Klinger, D.; Krogstad, D. V.; Kim, B. J.; Cameron, A.; Kim, S.-W.; Delaney, K. T.; Hur, S.-M.; Killops, K. L.; Fredrickson, G. H.; Kramer, E. J.; Hawker, C. J. *Journal of the American Chemical Society* **2013,** 135, (17), 6649-6657.
70. Deng, R.; Liang, F.; Zhou, P.; Zhang, C.; Qu, X.; Wang, Q.; Li, J.; Zhu, J.; Yang, Z. *Advanced Materials* **2014,** 26, (26), 4469-4472.

71. Jia, L.; Albouy, P.-A.; Di Cicco, A.; Cao, A.; Li, M.-H. *Polymer* **2011,** 52, (12), 2565-2575.
72. Yang, H.; Jia, L.; Zhu, C.; Di-Cicco, A.; Levy, D.; Albouy, P.-A.; Li, M.-H.; Keller, P. *Macromolecules* **2010,** 43, (24), 10442-10451.
73. Jia, L.; Cao, A.; Levy, D.; Xu, B.; Albouy, P.-A.; Xing, X.; Bowick, M. J.; Li, M.-H. *Soft Matter* **2009,** 5, (18), 3446-3451.
74. Christian, D. A.; Tian, A.; Ellenbroek, W. G.; Levental, I.; Rajagopal, K.; Janmey, P. A.; Liu, A. J.; Baumgart, T.; Discher, D. E. *Nat Mater* **2009,** 8, (10), 843-849.
75. Löbling, T. I.; Haataja, J. S.; Synatschke, C. V.; Schacher, F. H.; Müller, M.; Hanisch, A.; Gröschel, A. H.; Müller, A. H. E. *ACS Nano* **2014,** 8, (11), 11330-11340.
76. Schacher, F.; Walther, A.; Müller, A. H. E. *Langmuir* **2009,** 25, (18), 10962-10969.
77. Schacher, F.; Betthausen, E.; Walther, A.; Schmalz, H.; Pergushov, D. V.; Müller, A. H. E. *ACS Nano* **2009,** 3, (8), 2095-2102.
78. Synatschke, C. V.; Löbling, T. I.; Förtsch, M.; Hanisch, A.; Schacher, F. H.; Müller, A. H. E. *Macromolecules* **2013,** 46, (16), 6466-6474.
79. Synatschke, C. V.; Schacher, F. H.; Fortsch, M.; Drechsler, M.; Muller, A. H. E. *Soft Matter* **2011,** 7, (5), 1714-1725.
80. Gröschel, A. H.; Schacher, F. H.; Schmalz, H.; Borisov, O. V.; Zhulina, E. B.; Walther, A.; Müller, A. H. E. *Nature Communications* **2012,** 3, 710.
81. Groschel, A. H.; Walther, A.; Lobling, T. I.; Schacher, F. H.; Schmalz, H.; Muller, A. H. E. *Nature* **2013,** 503, (7475), 247-251.
82. Kim, J.-H.; Kwon, W. J.; Sohn, B.-H. *Chemical Communications* **2015,** 51, (16), 3324-3327.
83. Walther, A.; Barner-Kowollik, C.; Müller, A. H. E. *Langmuir* **2010,** 26, (14), 12237-12246.
84. Cui, H.; Chen, Z.; Zhong, S.; Wooley, K. L.; Pochan, D. J. *Science* **2007,** 317, (5838), 647-650.
85. Zhu, J.; Zhang, S.; Zhang, K.; Wang, X.; Mays, J. W.; Wooley, K. L.; Pochan, D. J. *Nature Communications* **2013,** 4, 2297.
86. Wang, Y.; Hollingsworth, A. D.; Yang, S. K.; Patel, S.; Pine, D. J.; Weck, M. *Journal of the American Chemical Society* **2013,** 135, (38), 14064-14067.
87. Winter, A.; Hager, M. D.; Newkome, G. R.; Schubert, U. S. *Advanced Materials* **2011,** 23, (48), 5728-5748.
88. Gohy, J.-F.; Lohmeijer, B. G. G.; Varshney, S. K.; Décamps, B.; Leroy, E.; Boileau, S.; Schubert, U. S. *Macromolecules* **2002,** 35, (26), 9748-9755.
89. Uchman, M.; Štěpánek, M.; Procházka, K.; Mountrichas, G.; Pispas, S.; Voets, I. K.; Walther, A. *Macromolecules* **2009,** 42, (15), 5605-5613.
90. Zheng, R.; Liu, G.; Yan, X. *Journal of the American Chemical Society* **2005,** 127, (44), 15358-15359.
91. Hu, J.; Liu, G. *Macromolecules* **2005,** 38, (19), 8058-8065.
92. Yan, X.; Liu, G.; Hu, J.; Willson, C. G. *Macromolecules* **2006,** 39, (5), 1906-1912.
93. Dupont, J.; Liu, G. *Soft Matter* **2010,** 6, (15), 3654-3661.
94. Lotz, B.; Kovacs, A. J.; Bassett, G. A.; Keller, A. *Kolloid-Zeitschrift und Zeitschrift für Polymere* **1966,** 209, (2), 115-128.
95. Lotz, B.; Kovacs, A. J. *Kolloid-Zeitschrift und Zeitschrift für Polymere* **1966,** 209, (2), 97-114.
96. Gast, A. P.; Vinson, P. K.; Cogan-Farinas, K. A. *Macromolecules* **1993,** 26, (7), 1774-1776.
97. Lin, E. K.; Gast, A. P. *Macromolecules* **1996,** 29, (12), 4432-4441.
98. Vilgis, T.; Halperin, A. *Macromolecules* **1991,** 24, (8), 2090-2095.
99. He, W.-N.; Xu, J.-T. *Progress in Polymer Science* **2012,** 37, (10), 1350-1400.
100. Qian, J.; Zhang, M.; Manners, I.; Winnik, M. A. *Trends in Biotechnology* **2010,** 28, (2), 84-92.
101. Hailes, R. L. N.; Oliver, A. M.; Gwyther, J.; Whittell, G. R.; Manners, I. *Chemical Society Reviews* **2016,** 45, (19), 5358-5407.
102. Massey, J. A.; Temple, K.; Cao, L.; Rharbi, Y.; Raez, J.; Winnik, M. A.; Manners, I. *Journal of the American Chemical Society* **2000,** 122, (47), 11577-11584.
103. Cao, L.; Manners, I.; Winnik, M. A. *Macromolecules* **2002,** 35, (22), 8258-8260.

104. Patra, S. K.; Ahmed, R.; Whittell, G. R.; Lunn, D. J.; Dunphy, E. L.; Winnik, M. A.; Manners, I. *Journal of the American Chemical Society* **2011,** 133, (23), 8842-8845.
105. Gwyther, J.; Gilroy, J. B.; Rupar, P. A.; Lunn, D. J.; Kynaston, E.; Patra, S. K.; Whittell, G. R.; Winnik, M. A.; Manners, I. *Chemistry – A European Journal* **2013,** 19, (28), 9186-9197.
106. Qian, J.; Li, X.; Lunn, D. J.; Gwyther, J.; Hudson, Z. M.; Kynaston, E.; Rupar, P. A.; Winnik, M. A.; Manners, I. *Journal of the American Chemical Society* **2014,** 136, (11), 4121-4124.
107. Kamps, A. C.; Fryd, M.; Park, S.-J. *ACS Nano* **2012,** 6, (3), 2844-2852.
108. Park, S.-J.; Kang, S.-G.; Fryd, M.; Saven, J. G.; Park, S.-J. *Journal of the American Chemical Society* **2010,** 132, (29), 9931-9933.
109. Lee, E.; Hammer, B.; Kim, J.-K.; Page, Z.; Emrick, T.; Hayward, R. C. *Journal of the American Chemical Society* **2011,** 133, (27), 10390-10393.
110. Petzetakis, N.; Dove, A. P.; O'Reilly, R. K. *Chemical Science* **2011,** 2, (5), 955-960.
111. Petzetakis, N.; Walker, D.; Dove, A. P.; O'Reilly, R. K. *Soft Matter* **2012,** 8, (28), 7408-7414.
112. Sun, L.; Petzetakis, N.; Pitto-Barry, A.; Schiller, T. L.; Kirby, N.; Keddie, D. J.; Boyd, B. J.; O'Reilly, R. K.; Dove, A. P. *Macromolecules* **2013,** 46, (22), 9074-9082.
113. Fu, J.; Luan, B.; Yu, X.; Cong, Y.; Li, J.; Pan, C.; Han, Y.; Yang, Y.; Li, B. *Macromolecules* **2004,** 37, (3), 976-986.
114. He, W.-N.; Zhou, B.; Xu, J.-T.; Du, B.-Y.; Fan, Z.-Q. *Macromolecules* **2012,** 45, (24), 9768-9778.
115. Du, Z.-X.; Xu, J.-T.; Fan, Z.-Q. *Macromolecules* **2007,** 40, (21), 7633-7637.
116. Mihut, A. M.; Drechsler, M.; Möller, M.; Ballauff, M. *Macromolecular Rapid Communications* **2010,** 31, (5), 449-453.
117. Schmelz, J.; Schedl, A. E.; Steinlein, C.; Manners, I.; Schmalz, H. *Journal of the American Chemical Society* **2012,** 134, (34), 14217-14225.
118. Yin, L.; Lodge, T. P.; Hillmyer, M. A. *Macromolecules* **2012,** 45, (23), 9460-9467.
119. Schmalz, H.; Schmelz, J.; Drechsler, M.; Yuan, J.; Walther, A.; Schweimer, K.; Mihut, A. M. *Macromolecules* **2008,** 41, (9), 3235-3242.
120. Schöbel, J.; Karg, M.; Rosenbach, D.; Krauss, G.; Greiner, A.; Schmalz, H. *Macromolecules* **2016,** 49, (7), 2761-2771.
121. Lazzari, M.; Scalarone, D.; Vazquez-Vazquez, C.; López-Quintela, M. A. *Macromolecular Rapid Communications* **2008,** 29, (4), 352-357.
122. Gadt, T.; Ieong, N. S.; Cambridge, G.; Winnik, M. A.; Manners, I. *Nat Mater* **2009,** 8, (2), 144-150.
123. Gädt, T.; Schacher, F. H.; McGrath, N.; Winnik, M. A.; Manners, I. *Macromolecules* **2011,** 44, (10), 3777-3786.
124. Du, V. A.; Qiu, H.; Winnik, M. A.; Whittell, G. R.; Manners, I. *Macromolecular Chemistry and Physics* **2016,** 217, (15), 1671-1682.
125. Zhang, J.; Wang, L.-Q.; Wang, H.; Tu, K. *Biomacromolecules* **2006,** 7, (9), 2492-500.
126. Li, X.; Jin, B.; Gao, Y.; Hayward, D. W.; Winnik, M. A.; Luo, Y.; Manners, I. *Angewandte Chemie International Edition* **2016,** 55, (38), 11392-11396.
127. Gao, Y.; Li, X.; Hong, L.; Liu, G. *Macromolecules* **2012,** 45, (3), 1321-1330.
128. Jia, L.; Levy, D.; Durand, D.; Imperor-Clerc, M.; Cao, A.; Li, M.-H. *Soft Matter* **2011,** 7, (16), 7395-7403.
129. Yoon, K.-Y.; Lee, I.-H.; Choi, T.-L. *RSC Advances* **2014,** 4, (90), 49180-49185.
130. Yoon, K.-Y.; Lee, I.-H.; Kim, K. O.; Jang, J.; Lee, E.; Choi, T.-L. *Journal of the American Chemical Society* **2012,** 134, (35), 14291-14294.
131. Lee, I.-H.; Amaladass, P.; Choi, T.-L. *Chemical Communications* **2014,** 50, (59), 7945-7948.
132. Kynaston, E. L.; Gould, O. E. C.; Gwyther, J.; Whittell, G. R.; Winnik, M. A.; Manners, I. *Macromolecular Chemistry and Physics* **2015,** 216, (6), 685-695.
133. Tung, Y.-C.; Wu, W.-C.; Chen, W.-C. *Macromolecular Rapid Communications* **2006,** 27, (21), 1838-1844.
134. Lin, C.-H.; Tung, Y.-C.; Ruokolainen, J.; Mezzenga, R.; Chen, W.-C. *Macromolecules* **2008,** 41, (22), 8759-8769.

135. Tian, Y.; Chen, C.-Y.; Yip, H.-L.; Wu, W.-C.; Chen, W.-C.; Jen, A. K.-Y. *Macromolecules* **2010,** 43, 282-291.
136. Li, K.; Wang, Q. *Chemical Communications* **2005**, (38), 4786-4788.
137. Leclère, P.; Calderone, A.; Marsitzky, D.; Francke, V.; Geerts, Y.; Müllen, K.; Brédas, J. L.; Lazzaroni, R. *Advanced Materials* **2000,** 12, (14), 1042-1046.
138. Urban, V.; Wang, H. H.; Thiyagarajan, P.; Littrell, K. C.; Wang, H. B.; Yu, L. *Journal of Applied Crystallography* **2000,** 33, (3 Part 1), 645-649.
139. Wang, H.; Wang, H. H.; Urban, V. S.; Littrell, K. C.; Thiyagarajan, P.; Yu, L. *Journal of the American Chemical Society* **2000,** 122, (29), 6855-6861.
140. Wang, H.; You, W.; Jiang, P.; Yu, L.; Wang, H. H. *Chemistry – A European Journal* **2004,** 10, (4), 986-993.
141. Mori, T.; Watanabe, T.; Minagawa, K.; Tanaka, M. *Journal of Polymer Science Part A: Polymer Chemistry* **2005,** 43, (8), 1569-1578.
142. Feng, C.; Jose Gonzalez-Alvarez, M.; Song, Y.; Li, I.; Zhao, G.; Molev, G.; Guerin, G.; Walker, G.; Scholes, G. D.; Manners, I.; Winnik, M. A. *Soft Matter* **2014,** 10, (44), 8875-8887.
143. Lee, C.-U.; Smart, T. P.; Guo, L.; Epps, T. H.; Zhang, D. *Macromolecules* **2011,** 44, (24), 9574-9585.
144. Legros, C.; De Pauw-Gillet, M.-C.; Tam, K. C.; Taton, D.; Lecommandoux, S. *Soft Matter* **2015,** 11, (17), 3354-3359.
145. Hudson, Z. M.; Boott, C. E.; Robinson, M. E.; Rupar, P. A.; Winnik, M. A.; Manners, I. *Nat Chem* **2014,** 6, (10), 893-898.
146. Schmelz, J.; Karg, M.; Hellweg, T.; Schmalz, H. *ACS Nano* **2011,** 5, 9523-9523.
147. Hsiao, M.-S.; Yusoff, S. F. M.; Winnik, M. A.; Manners, I. *Macromolecules* **2014,** 47, (7), 2361-2372.
148. Sun, L.; Pitto-Barry, A.; Kirby, N.; Schiller, T. L.; Sanchez, A. M.; Dyson, M. A.; Sloan, J.; Wilson, N. R.; O'Reilly, R. K.; Dove, A. P. *Nature Communications* **2014,** 5, 5746.
149. Wang, X.; Guerin, G.; Wang, H.; Wang, Y.; Manners, I.; Winnik, M. A. *Science* **2007,** 317, (5838), 644-647.
150. Gilroy, J. B.; Rupar, P. A.; Whittell, G. R.; Chabanne, L.; Terrill, N. J.; Winnik, M. A.; Manners, I.; Richardson, R. M. *Journal of the American Chemical Society* **2011,** 133, (42), 17056-17062.
151. Gilroy, J. B.; Gädt, T.; Whittell, G. R.; Chabanne, L.; Mitchels, J. M.; Richardson, R. M.; Winnik, M. A.; Manners, I. *Nat Chem* **2010,** 2, (7), 566-570.
152. Qian, J.; Lu, Y.; Cambridge, G.; Guerin, G.; Manners, I.; Winnik, M. A. *Macromolecules* **2012,** 45, (20), 8363-8372.
153. Qian, J.; Lu, Y.; Chia, A.; Zhang, M.; Rupar, P. A.; Gunari, N.; Walker, G. C.; Cambridge, G.; He, F.; Guerin, G.; Manners, I.; Winnik, M. A. *ACS Nano* **2013,** 7, (5), 3754-3766.
154. Rupar, P. A.; Chabanne, L.; Winnik, M. A.; Manners, I. *Science* **2012,** 337, (6094), 559-562.
155. Qiu, H.; Gao, Y.; Du, V. A.; Harniman, R.; Winnik, M. A.; Manners, I. *Journal of the American Chemical Society* **2015,** 137, (6), 2375-2385.
156. Qiu, H.; Russo, G.; Rupar, P. A.; Chabanne, L.; Winnik, M. A.; Manners, I. *Angewandte Chemie International Edition* **2012,** 51, (47), 11882-11885.
157. Qiu, H.; Hudson, Z. M.; Winnik, M. A.; Manners, I. *Science* **2015,** 347, (6228), 1329-1332.
158. Wang, H.; Lin, W.; Fritz, K. P.; Scholes, G. D.; Winnik, M. A.; Manners, I. *Journal of the American Chemical Society* **2007,** 129, (43), 12924-12925.
159. Nunns, A.; Whittell, G. R.; Winnik, M. A.; Manners, I. *Macromolecules* **2014,** 47, (23), 8420-8428.
160. Finnegan, J. R.; Lunn, D. J.; Gould, O. E. C.; Hudson, Z. M.; Whittell, G. R.; Winnik, M. A.; Manners, I. *Journal of the American Chemical Society* **2014,** 136, (39), 13835-13844.
161. Hudson, Z. M.; Lunn, D. J.; Winnik, M. A.; Manners, I. *Nature Communications* **2014,** 5, 3372.
162. Nazemi, A.; Boott, C. E.; Lunn, D. J.; Gwyther, J.; Hayward, D. W.; Richardson, R. M.; Winnik, M. A.; Manners, I. *Journal of the American Chemical Society* **2016,** 138, (13), 4484-4493.

163. Wittmann, J. C.; Lotz, B. *Journal of Polymer Science: Polymer Physics Edition* **1981,** 19, (12), 1837-1851.
164. Chen, W. Y.; Li, C. Y.; Zheng, J. X.; Huang, P.; Zhu, L.; Ge, Q.; Quirk, R. P.; Lotz, B.; Deng, L.; Wu, C.; Thomas, E. L.; Cheng, S. Z. D. *Macromolecules* **2004,** 37, (14), 5292-5299.
165. Zheng, J. X.; Xiong, H.; Chen, W. Y.; Lee, K.; Van Horn, R. M.; Quirk, R. P.; Lotz, B.; Thomas, E. L.; Shi, A.-C.; Cheng, S. Z. D. *Macromolecules* **2006,** 39, (2), 641-650.
166. Wang, J.; Zhu, W.; Peng, B.; Chen, Y. *Polymer* **2013,** 54, (25), 6760-6767.
167. Su, M.; Huang, H.; Ma, X.; Wang, Q.; Su, Z. *Macromolecular Rapid Communications* **2013,** 34, (13), 1067-1071.
168. Mohd Yusoff, S. F.; Hsiao, M.-S.; Schacher, F. H.; Winnik, M. A.; Manners, I. *Macromolecules* **2012,** 45, (9), 3883-3891.
169. Wang, Z.; Cao, Y.; Song, J.; Xie, Z.; Wang, Y. *Langmuir* **2016,** 32, (37), 9633-9639.
170. Wu, J.; Weng, L.-T.; Qin, W.; Liang, G.; Tang, B. Z. *ACS Macro Letters* **2015,** 4, (5), 593-597.
171. Li, Z.; Liu, R.; Mai, B.; Wang, W.; Wu, Q.; Liang, G.; Gao, H.; Zhu, F. *Polymer* **2013,** 54, (6), 1663-1670.
172. Qiu, H.; Gao, Y.; Boott, C. E.; Gould, O.; Harniman, R. L.; Richardson, R. M.; Miles, M. J.; Manners, I. *Science* **2016,** 352, (6286), 697-697.
173. Yu, B.; Jiang, X.; Yin, J. *Macromolecules* **2014,** 47, (14), 4761-4768.
174. Rupar, P. A.; Cambridge, G.; Winnik, M. A.; Manners, I. *Journal of the American Chemical Society* **2011,** 133, (42), 16947-16957.
175. Qiu, H.; Cambridge, G.; Winnik, M. A.; Manners, I. *Journal of the American Chemical Society* **2013,** 135, (33), 12180-3.
176. Jia, L.; Zhao, G.; Shi, W.; Coombs, N.; Gourevich, I.; Walker, G. C.; Guerin, G.; Manners, I.; Winnik, M. A. *Nature Communications* **2014,** 5, 3882.
177. Jia, L.; Petretic, A.; Molev, G.; Guerin, G.; Manners, I.; Winnik, M. A. *ACS Nano* **2015,** 9, (11), 10673-10685.
178. Gao, Y.; Qiu, H.; Zhou, H.; Li, X.; Harniman, R.; Winnik, M. A.; Manners, I. *Journal of the American Chemical Society* **2015,** 137, (6), 2203-2206.
179. Wang, H.; Patil, A. J.; Liu, K.; Petrov, S.; Mann, S.; Winnik, M. A.; Manners, I. *Advanced Materials* **2009,** 21, (18), 1805-1808.
180. McGrath, N.; Patil, A. J.; Watson, S. M. D.; Horrocks, B. R.; Faul, C. F. J.; Houlton, A.; Winnik, M. A.; Mann, S.; Manners, I. *Chemistry – A European Journal* **2013,** 19, (39), 13030-13039.
181. Li, X.; Gao, Y.; Boott, C. E.; Winnik, M. A.; Manners, I. *Nature Communications* **2015,** 6, 8127.
182. Li, X.; Gao, Y.; Boott, C. E.; Hayward, D. W.; Harniman, R.; Whittell, G. R.; Richardson, R. M.; Winnik, M. A.; Manners, I. *Journal of the American Chemical Society* **2016,** 138, (12), 4087-95.
183. Li, X.; Gao, Y.; Boott, C. E.; Hayward, D. W.; Harniman, R.; Whittell, G. R.; Richardson, R. M.; Winnik, M. A.; Manners, I. *Journal of the American Chemical Society* **2016,** 138, 4087-95.
184. Canning, S. L.; Smith, G. N.; Armes, S. P. *Macromolecules* **2016,** 49, (6), 1985-2001.
185. Jennings, J.; Beija, M.; Kennon, J. T.; Willcock, H.; O'Reilly, R. K.; Rimmer, S.; Howdle, S. M. *Macromolecules* **2013,** 46, (17), 6843-6851.
186. Jennings, J.; Beija, M.; Richez, A. P.; Cooper, S. D.; Mignot, P. E.; Thurecht, K. J.; Jack, K. S.; Howdle, S. M. *Journal of the American Chemical Society* **2012,** 134, (10), 4772-4781.
187. Zhang, Q.; Zhu, S. *ACS Macro Letters* **2015,** 4, (7), 755-758.
188. Lowe, A. B. *Polymer* **2016,** 106, 161-181.
189. Delaittre, G.; Nicolas, J.; Lefay, C.; Save, M.; Charleux, B. *Chemical Communications* **2005**, (5), 614-616.
190. Groison, E.; Brusseau, S.; D'Agosto, F.; Magnet, S.; Inoubli, R.; Couvreur, L.; Charleux, B. *ACS Macro Letters* **2012,** 1, (1), 47-51.
191. Wan, W.-M.; Pan, C.-Y. *Macromolecules* **2007,** 40, (25), 8897-8905.
192. Rieger, J.; Osterwinter, G.; Bui, C.; Stoffelbach, F.; Charleux, B. *Macromolecules* **2009,** 42, (15), 5518-5525.

193. Boursier, T.; Chaduc, I.; Rieger, J.; D'Agosto, F.; Lansalot, M.; Charleux, B. *Polymer Chemistry* **2011,** 2, (2), 355-362.
194. An, Z.; Shi, Q.; Tang, W.; Tsung, C.-K.; Hawker, C. J.; Stucky, G. D. *Journal of the American Chemical Society* **2007,** 129, (46), 14493-14499.
195. An, Z.; Tang, W.; Hawker, C. J.; Stucky, G. D. *Journal of the American Chemical Society* **2006,** 128, (47), 15054-15055.
196. Grazon, C.; Rieger, J.; Sanson, N.; Charleux, B. *Soft Matter* **2011,** 7, (7), 3482-3490.
197. Delaittre, G.; Save, M.; Charleux, B. *Macromolecular Rapid Communications* **2007,** 28, (15), 1528-1533.
198. Rieger, J.; Grazon, C.; Charleux, B.; Alaimo, D.; Jérôme, C. *Journal of Polymer Science Part A: Polymer Chemistry* **2009,** 47, (9), 2373-2390.
199. Liu, G.; Qiu, Q.; An, Z. *Polymer Chemistry* **2012,** 3, (2), 504-513.
200. Liu, G.; Qiu, Q.; Shen, W.; An, Z. *Macromolecules* **2011,** 44, (13), 5237-5245.
201. Blanazs, A.; Ryan, A. J.; Armes, S. P. *Macromolecules* **2012,** 45, (12), 5099-5107.
202. Blanazs, A.; Madsen, J.; Battaglia, G.; Ryan, A. J.; Armes, S. P. *Journal of the American Chemical Society* **2011,** 133, (41), 16581-16587.
203. Shen, W.; Chang, Y.; Liu, G.; Wang, H.; Cao, A.; An, Z. *Macromolecules* **2011,** 44, (8), 2524-2530.
204. Chambon, P.; Blanazs, A.; Battaglia, G.; Armes, S. P. *Macromolecules* **2012,** 45, (12), 5081-5090.
205. Jones, E. R.; Mykhaylyk, O. O.; Semsarilar, M.; Boerakker, M.; Wyman, P.; Armes, S. P. *Macromolecules* **2016,** 49, (1), 172-181.
206. Zehm, D.; Ratcliffe, L. P. D.; Armes, S. P. *Macromolecules* **2013,** 46, (1), 128-139.
207. Zhang, X.; Boisse, S.; Bui, C.; Albouy, P.-A.; Brulet, A.; Li, M.-H.; Rieger, J.; Charleux, B. *Soft Matter* **2012,** 8, (4), 1130-1141.
208. Semsarilar, M.; Penfold, N. J. W.; Jones, E. R.; Armes, S. P. *Polymer Chemistry* **2015,** 6, (10), 1751-1757.
209. Lee, I.-H.; Amaladass, P.; Yoon, K.-Y.; Shin, S.; Kim, Y.-J.; Kim, I.; Lee, E.; Choi, T.-L. *Journal of the American Chemical Society* **2013,** 135, (47), 17695-17698.
210. Boott, C. E.; Gwyther, J.; Harniman, R. L.; Hayward, D. W.; Manners, I. *In press* **2016**.
211. Discher, B. M.; Won, Y.-Y.; Ege, D. S.; Lee, J. C.-M.; Bates, F. S.; Discher, D. E.; Hammer, D. A. *Science* **1999,** 284, (5417), 1143-1146.
212. Brinkhuis, R. P.; Rutjes, F. P. J. T.; van Hest, J. C. M. *Polymer Chemistry* **2011,** 2, (7), 1449-1462.
213. Elsabahy, M.; Wooley, K. L. *Chemical Society Reviews* **2012,** 41, (7), 2545-2561.
214. Movassaghian, S.; Merkel, O. M.; Torchilin, V. P. *Wiley Interdisciplinary Reviews: Nanomedicine and Nanobiotechnology* **2015,** 7, (5), 691-707.
215. Herzberger, J.; Niederer, K.; Pohlit, H.; Seiwert, J.; Worm, M.; Wurm, F. R.; Frey, H. *Chemical Reviews* **2016,** 116, (4), 2170-2243.
216. Alakhova, D. Y.; Kabanov, A. V. *Molecular Pharmaceutics* **2014,** 11, (8), 2566-2578.
217. Ahmed, F.; Pakunlu, R. I.; Brannan, A.; Bates, F.; Minko, T.; Discher, D. E. *Journal of Controlled Release* **2006,** 116, (2), 150-158.
218. Ahmed, F.; Pakunlu, R. I.; Srinivas, G.; Brannan, A.; Bates, F.; Klein, M. L.; Minko, T.; Discher, D. E. *Molecular Pharmaceutics* **2006,** 3, (3), 340-350.
219. Du, Z.-X.; Xu, J.-T.; Fan, Z.-Q. *Macromolecules* **2007,** 40, (21), 7633-7637.
220. Rizis, G.; van de Ven, T. G. M.; Eisenberg, A. *Soft Matter* **2014,** 10, (16), 2825-2835.
221. Rizis, G.; van de Ven, T. G. M.; Eisenberg, A. *ACS Nano* **2015,** 9, (4), 3627-3640.
222. Sun, L.; Petzetakis, N.; Pitto-Barry, A.; Schiller, T. L.; Kirby, N.; Keddie, D. J.; Boyd, B. J.; O'Reilly, R. K.; Dove, A. P. *Macromolecules* **2013,** 46, (22), 9074-9082.
223. Pitto-Barry, A.; Kirby, N.; Dove, A. P.; O'Reilly, R. K. *Polymer Chemistry* **2014,** 5, (4), 1427-1436.

224. Nasongkla, N.; Bey, E.; Ren, J.; Ai, H.; Khemtong, C.; Guthi, J. S.; Chin, S.-F.; Sherry, A. D.; Boothman, D. A.; Gao, J. *Nano Letters* **2006,** 6, (11), 2427-2430.
225. Dekker, C. *Nat Nano* **2007,** 2, (4), 209-215.
226. Zhang, K.; Fang, H.; Chen, Z.; Taylor, J.-S. A.; Wooley, K. L. *Bioconjugate Chemistry* **2008,** 19, (9), 1880-1887.
227. Zhang, K.; Rossin, R.; Hagooly, A.; Chen, Z.; Welch, M. J.; Wooley, K. L. *Journal of Polymer Science Part A: Polymer Chemistry* **2008,** 46, (22), 7578-7583.
228. Karagoz, B.; Esser, L.; Duong, H. T.; Basuki, J. S.; Boyer, C.; Davis, T. P. *Polymer Chemistry* **2014,** 5, (2), 350-355.
229. Harada, A.; Kataoka, K. *Progress in Polymer Science* **2006,** 31, (11), 949-982.
230. Ladmiral, V.; Semsarilar, M.; Canton, I.; Armes, S. P. *Journal of the American Chemical Society* **2013,** 135, (36), 13574-13581.
231. Jo, Y. S.; van der Vlies, A. J.; Gantz, J.; Thacher, T. N.; Antonijevic, S.; Cavadini, S.; Demurtas, D.; Stergiopulos, N.; Hubbell, J. A. *Journal of the American Chemical Society* **2009,** 131, (40), 14413-14418.
232. Hasegawa, U.; van der Vlies, A. J.; Simeoni, E.; Wandrey, C.; Hubbell, J. A. *Journal of the American Chemical Society* **2010,** 132, (51), 18273-18280.
233. Pisoni, R. L.; Acker, T. L.; Lisowski, K. M.; Lemons, R. M.; Thoene, J. G. *The Journal of Cell Biology* **1990,** 110, (2), 327-335.
234. Lloyd, J. B. *Biochemical Journal* **1986,** 237, (1), 271-272.
235. Li, Y.; Hindi, K.; Watts, K. M.; Taylor, J. B.; Zhang, K.; Li, Z.; Hunstad, D. A.; Cannon, C. L.; Youngs, W. J.; Wooley, K. L. *Chemical Communications* **2010,** 46, (1), 121-123.
236. Williams, M.; Penfold, N. J. W.; Lovett, J. R.; Warren, N. J.; Douglas, C. W. I.; Doroshenko, N.; Verstraete, P.; Smets, J.; Armes, S. P. *Polymer Chemistry* **2016,** 7, (23), 3864-3873.
237. Stuart, M. A. C.; Huck, W. T. S.; Genzer, J.; Muller, M.; Ober, C.; Stamm, M.; Sukhorukov, G. B.; Szleifer, I.; Tsukruk, V. V.; Urban, M.; Winnik, F.; Zauscher, S.; Luzinov, I.; Minko, S. *Nat Mater* **2010,** 9, (2), 101-113.
238. Roy, D.; Brooks, W. L. A.; Sumerlin, B. S. *Chemical Society Reviews* **2013,** 42, (17), 7214-7243.
239. Pei, Y.; Dharsana, N. C.; van Hensbergen, J. A.; Burford, R. P.; Roth, P. J.; Lowe, A. B. *Soft Matter* **2014,** 10, (31), 5787-5796.
240. Fielding, L. A.; Lane, J. A.; Derry, M. J.; Mykhaylyk, O. O.; Armes, S. P. *Journal of the American Chemical Society* **2014,** 136, (15), 5790-5798.
241. Blanazs, A.; Verber, R.; Mykhaylyk, O. O.; Ryan, A. J.; Heath, J. Z.; Douglas, C. W. I.; Armes, S. P. *Journal of the American Chemical Society* **2012,** 134, (23), 9741-9748.
242. Mitchell, D. E.; Lovett, J. R.; Armes, S. P.; Gibson, M. I. *Angewandte Chemie International Edition* **2016,** 55, (8), 2801-2804.
243. Kim, K. T.; Park, C.; Vandermeulen, G. W. M.; Rider, D. A.; Kim, C.; Winnik, M. A.; Manners, I. *Angewandte Chemie International Edition* **2005,** 44, (48), 7964-7968.
244. Wang, G.; Tong, X.; Zhao, Y. *Macromolecules* **2004,** 37, (24), 8911-8917.
245. Power-Billard, K. N.; Spontak, R. J.; Manners, I. *Angewandte Chemie International Edition* **2004,** 43, (10), 1260-1264.
246. Eloi, J.-C.; Rider, D. A.; Cambridge, G.; Whittell, G. R.; Winnik, M. A.; Manners, I. *Journal of the American Chemical Society* **2011,** 133, (23), 8903-8913.
247. Wang, H.; Wang, X.; Winnik, M. A.; Manners, I. *Journal of the American Chemical Society* **2008,** 130, (39), 12921-12930.
248. Schmidt, B. V. K. J.; Elbert, J.; Scheid, D.; Hawker, C. J.; Klinger, D.; Gallei, M. *ACS Macro Letters* **2015,** 4, (7), 731-735.
249. Kim, Y.-Y.; Ganesan, K.; Yang, P.; Kulak, A. N.; Borukhin, S.; Pechook, S.; Ribeiro, L.; Kröger, R.; Eichhorn, S. J.; Armes, S. P.; Pokroy, B.; Meldrum, F. C. *Nat Mater* **2011,** 10, (11), 890-896.
250. Rae Cho, K.; Kim, Y.-Y.; Yang, P.; Cai, W.; Pan, H.; Kulak, A. N.; Lau, J. L.; Kulshreshtha, P.; Armes, S. P.; Meldrum, F. C.; De Yoreo, J. J. *Nature Communications* **2016,** 7, 10187.

251. Ning, Y.; Fielding, L. A.; Ratcliffe, L. P. D.; Wang, Y.-W.; Meldrum, F. C.; Armes, S. P. *Journal of the American Chemical Society* **2016,** 138, (36), 11734-11742.
252. Kim, H.-C.; Park, S.-M.; Hinsberg, W. D. *Chemical Reviews* **2010,** 110, (1), 146-177.
253. Galatsis, K.; Wang, K. L.; Ozkan, M.; Ozkan, C. S.; Huang, Y.; Chang, J. P.; Monbouquette, H. G.; Chen, Y.; Nealey, P.; Botros, Y. *Advanced Materials* **2010,** 22, (6), 769-778.
254. Bang, J.; Jeong, U.; Ryu, D. Y.; Russell, T. P.; Hawker, C. J. *Advanced Materials* **2009,** 21, (47), 4769-4792.
255. Cao, L.; Massey, J. A.; Winnik, M. A.; Manners, I.; Riethmüller, S.; Banhart, F.; Spatz, J. P.; Möller, M. *Advanced Functional Materials* **2003,** 13, (4), 271-276.
256. Kim, Y.-J.; Cho, C.-H.; Paek, K.; Jo, M.; Park, M.-k.; Lee, N.-E.; Kim, Y.-j.; Kim, B. J.; Lee, E. *Journal of the American Chemical Society* **2014,** 136, (7), 2767-2774.
257. Jin, S.-M.; Kim, I.; Lim, J. A.; Ahn, H.; Lee, E. *Advanced Functional Materials* **2016,** 26, (19), 3226-3235.
258. Ren, G.; Wu, P.-T.; Jenekhe, S. A. *ACS Nano* **2011,** 5, (1), 376-384.
259. Derry, M. J.; Fielding, L. A.; Armes, S. P. *Polymer Chemistry* **2015,** 6, (16), 3054-3062.
260. Zheng, R.; Liu, G.; Devlin, M.; Hux, K.; Jao, T.-C. *Tribol. Trans* **2010,** 53, 97-107.
261. Moad, G.; Rizzardo, E.; Thang, S. H. *Chemistry – An Asian Journal* **2013,** 8, (8), 1634-1644.
262. Hill, M. R.; Carmean, R. N.; Sumerlin, B. S. *Macromolecules* **2015,** 48, (16), 5459-5469.
263. Dean, J. M.; Verghese, N. E.; Pham, H. Q.; Bates, F. S. *Macromolecules* **2003,** 36, (25), 9267-9270.
264. Thio, Y. S.; Wu, J.; Bates, F. S. *Macromolecules* **2006,** 39, (21), 7187-7189.
265. Thompson, K. L.; Fielding, L. A.; Mykhaylyk, O. O.; Lane, J. A.; Derry, M. J.; Armes, S. P. *Chemical Science* **2015,** 6, (7), 4207-4214.
266. Thompson, K. L.; Mable, C. J.; Lane, J. A.; Derry, M. J.; Fielding, L. A.; Armes, S. P. *Langmuir* **2015,** 31, (14), 4137-4144.
267. Thompson, K. L.; Lane, J. A.; Derry, M. J.; Armes, S. P. *Langmuir* **2015,** 31, (15), 4373-4376.
268. La, Y.; Park, C.; Shin, T. J.; Joo, S. H.; Kang, S.; Kim, K. T. *Nat Chem* **2014,** 6, (6), 534-541.
269. Park, C.; La, Y.; An, T. H.; Jeong, H. Y.; Kang, S.; Joo, S. H.; Ahn, H.; Shin, T. J.; Kim, K. T. *Nature Communications* **2015,** 6, 6392.
270. Yu, H.; Qiu, X.; Nunes, S. P.; Peinemann, K.-V. *Nature Communications* **2014,** 5, 4110.
271. An, T. H.; La, Y.; Cho, A.; Jeong, M. G.; Shin, T. J.; Park, C.; Kim, K. T. *ACS Nano* **2015,** 9, (3), 3084-3096.

Table of Contents Entry

Perspective:

Functional Nanoparticles from the Solution Self-Assembly of Block Copolymers

Ulrich Tritschler, Sam Pearce, Jessica Gwyther, George Whittell, and Ian Manners*